Agrofood byproducts redirected towards Novel Sustainable Sunscreen applications

Mitra Karimpour Nahari
Master in Biochemistry
Department of FCUP and ICBAS
2023

Supervisor
Iva Fernandes, Assistant Professor, Faculty of Sciences of University of Porto

Co-supervisor
Nuno Mateus, Associate Professor, Faculty of Sciences of University of Porto

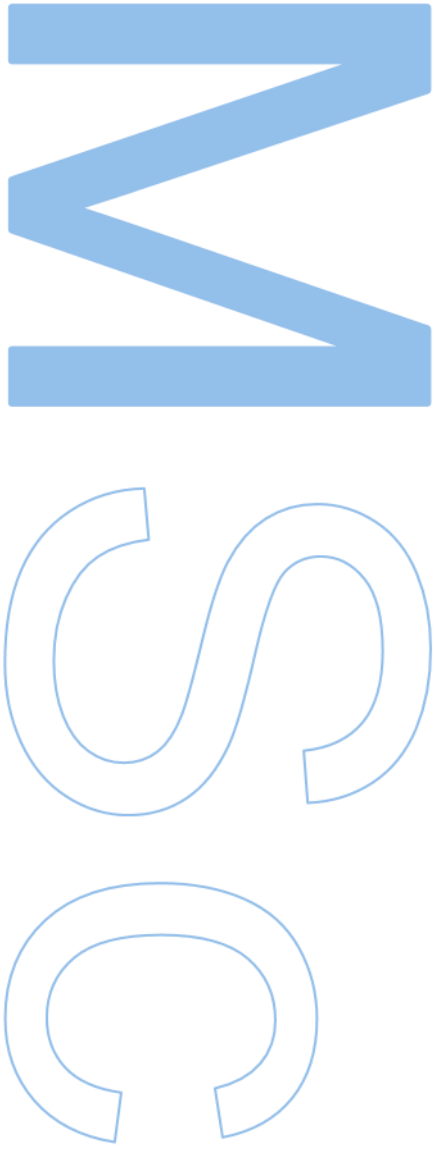


U.PORTO
INSTITUTO DE CIÊNCIAS
BIOMÉDICAS ABEL SALAZAR
UNIVERSIDADE DO PORTO

U.PORTO
FACULDADE DE CIÊNCIAS
UNIVERSIDADE DO PORTO

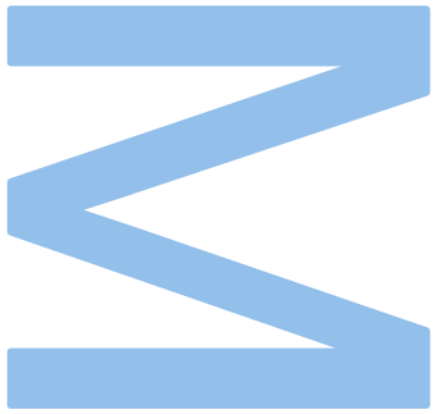

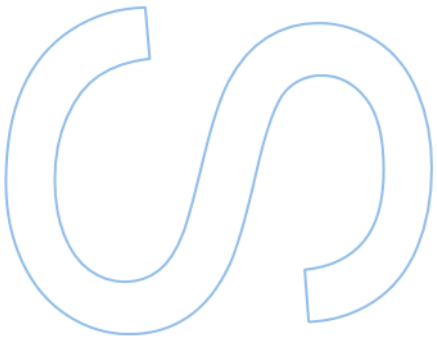

Acknowledgements

I would first like to express my sincere gratitude to my thesis advisor, Dra Iva Fernandes, who gave me an opportunity to do this dissertation. I would like to thank for her continuous support of my master study, her patience and motivation since the dissertation started until successful. Her guidance has been a great help in improvement of my dissertation.

I am also very grateful to my co-supervisors Professor Nuno Mateus, for the trust he placed in carrying out this work and constant dynamism, which allowed us to unlock stages and always move forward.

I would also thank to my laboratory colleagues. Especially Patricia Correia, who was very helpful with her knowledge and had an important role in the success of this dissertation.

Finally, I would like to thank my family for their continuous support and encouragement throughout my life.

Abstract

Organic sunscreen products, containing synthetic UV-filters, are used worldwide to protect from the harmful effects of sunlight. The replacement of these synthetic filters by natural solutions depends, among other features, on their photostability., Phenolic compounds, like anthocyanins shown to be excellent candidates as UV-filters, with additional antioxidant properties. Although their instability when exposed to light, oxygen, basic pHs and high temperatures, is a problem for skincare applications. Since, for promote and increasing the stability of these natural class of compounds, encapsulation or co-addition of different lignins was explored. At the end of this study, it was possible to select the co-addition of lignin sulfonate as the best approach, reaching formulations with a palette of different colours (with or without synthetic UV-filter), with improved stability, antioxidant features, non-toxic to skin cells, SPF values above 50 and rheological parameters similar to the original formulations.

In conclusion, it was possible to produce a range of innovative, sustainable and environmental friendly skincare cosmetics by upcycling agro-food industry by-products.

Key words:

UV rays, sunscreen, antioxidant, SPF, anthocyanidins, Cy3glc, lignin, Lignin sulfonates, blackberry, gel serum, nanoparticles, emulsion.

Table of Contents

List of Tables

List of Figures

List of Abbreviations

BB – blackberry extract

C – cy3glc

CLS - cell lines service

Cy3glc - cyanidin-3-o-glucoside

DLS - dynamic light scattering

DMSO - dimethyl sulfoxide

DPPH - 2,2-diphenyl-1-picrylhydrazyl

ELS - electrophoretic light scattering

IC_{50} - inhibitory concentration-50

KL – kraft lignin

LNP - lignin nanoparticles

LS - lignin sulfonate

NP – nanoparticles

PDI - polydispersity

Rmp - revolutions per minute

ROS – reactive oxygen species

SB - stratum basal

SC - stratum corneum

SG - stratum granulosum

SL - stratum lucidum

SPF – sun protection factor

SS - stratum spinous

TiO_2 - titanium dioxide

TEAC - trolox equivalent antioxidant capacity

UV – Ultraviolet

ZnO - Zinc Oxide

Introduction

1. Sunlight and Skin

Humans are constantly exposed to sunlight, whether that means simply being outdoors, participating in sports, or enjoying vacations in sunny locations. Although sunlight has beneficial effects such as vitamin D synthesis through ultraviolet B (UVB) radiation and lowering blood pressure, it also has consequences that endanger human health (Gernot Kunze, 2021). Sunlight is a continuous spectrum of electromagnetic radiation that is divided into three major spectrums of wavelength: ultraviolet, visible, and infrared. UV-light is classified as UVA, UVB, and UVC, according to wavelength range (**Table. 1**). UVA rays have the least energy among UV rays. UVB rays have slightly more energy than UVA rays. UVC rays have more energy than the other types of UV rays. Fortunately, because of this, they react with ozone high in our atmosphere and don't reach the ground, so they are not normally a risk factor for skin cancer (**Fig. 1**) (Yasuhiro Matsumura, 2003).

Table 1. UV classifications and their wavelength.

UV-classification	Wavelengths
UVA	(320-400 nm)
UVB	(280-320 nm)
UVC	(200-280 nm)

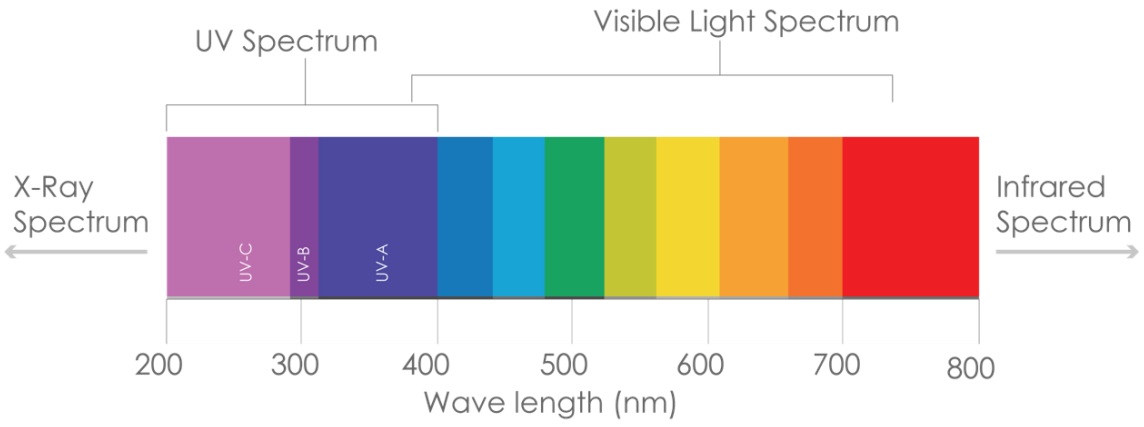

Fig. 1. UV radiation spectrum with certain wavelengths.

1.1. Health Effects Caused by UV-radiation

Skin has been recognized as the largest organ of the human body which has a major role in protecting the body from environmental stresses, such as water loss and microorganism infection, and is made up of three tissue layers: the epidermis, the dermis, and the hypodermis (**Fig. 2**). Hypodermis is the innermost layer of the skin that contains large amounts of fatty tissue. Also, nerves and connective tissue are located in this layer, which connects the skin to the underlying muscle and bone layer. The next layer, is dermis which forms the main and central part of the skin, containing skin cells, blood vessels, nerves, glands, and hair follicles and is much thicker in size than the epidermis. Likewise, fibroblasts, collagen, elastin, and hyaluronic acid polysaccharides are present in this layer, which provide strength and maintain elasticity and resilience of skin. The outermost layer of the skin is the epidermis which itself consists of several layers and different cells such as Melanocytes, Langerhans cells, Markel cells and mainly Keratinocytes, which produce the protein and keratin. Epidermis consists of 5 layers, which are, in order from the inside to the outside: 1) Stratum Basal (SB), which is the place of division and generation of keratinocytes; 2) Stratum Spinous (SS), which contains keratinocytes that have travelled upward from the basal layer; 3) Stratum Granulosum (SG), which contains keratinocytes that have travelled upward from the spinous layer. The keratinocytes present in this layer produce fats that constitute a barrier preventing dehydration by keeping water inside the skin; 4) Stratum Lucidum (SL), which is present only on the palms of hands and soles of feet; 5) Stratum Corneum (SC), which is the topmost layer of the epidermis that the keratinocyte cells of this layer, lost their alive contents, but instead are rich in keratin, which are firmly attached to each other. The SC layer is the body's primary line of defence against solar UV rays when exposed to sunlight. In addition, the SC layer provides mechanical protection of skin barrier to the external environment. Although the SC layer is typically a highly efficient barrier, exposure to rough conditions can change its function, leading to severe skin damage such as chapping and cracking. Therefore, this issue increases the risk of vulnerability of the lower layers of the skin (Anatomy and Physiology, 2013; Oktay Arda, 2014; Krysta Biniek, 2012).

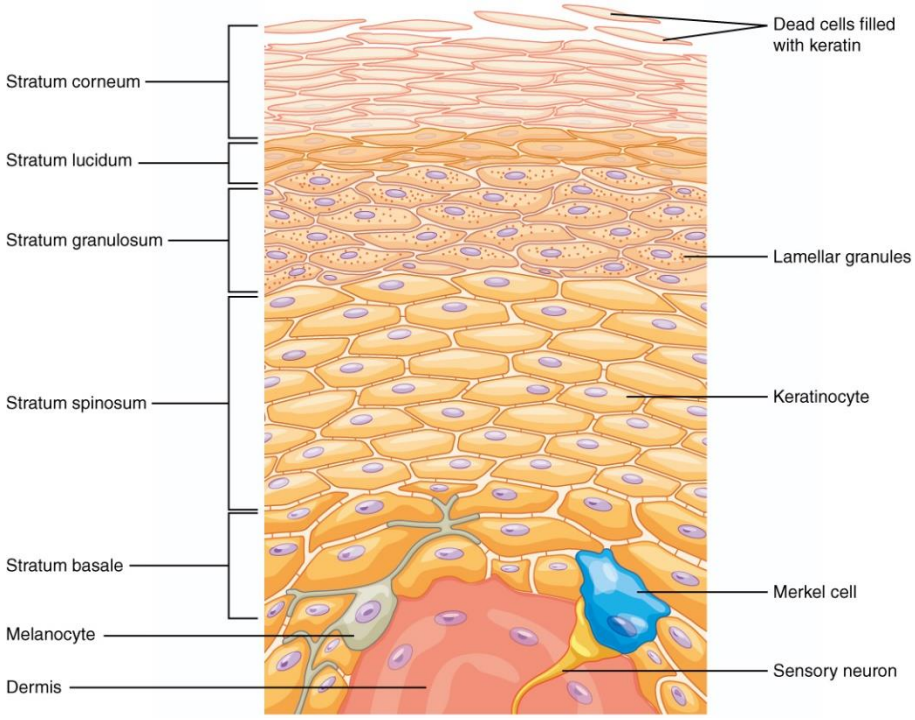

Fig. 2. The layers of epidermis (Anatomy and Physiology, 2013).

Skin, like all human organs, undergoes progressive alterations as a result of the passage of time, but unlike other organs, it is continuously exposed to harmful ultraviolet radiation (UVR) that leads to aftermath on the skin, such as photoaging, melanoma. In photo-aged skin, harmful sunlight induces the producing of free radicals in dermis fibroblast cells, on the one hand, inhibit the production of growth factors, preventing the production of collagen and elastin, and moreover, destroys dermis contents by activating collagen-destroying enzymes (matrix metalloproteinases or MMPS), elastin (elastase enzyme) and hyaluronic acid (hyaluronidase enzyme). Thus, the production of collagen decreases and the skin starts to lose elasticity causing to the formation of wrinkles (Jin Ho Chung, 2003; Yidong Tu, 2016). Moreover, UV rays can lead to an increase in the glycation mechanism in the cells, which is the covalent attachment of a sugar to a protein, lipid or nucleic acid molecule and these free sugars react with collagen and elastin protein fibers in the skin dermis and cause the formation of transverse connections between these fibers (AGEs) and their hardening. This process, causes the loss of skin elasticity and finally, the appearance of wrinkles in the skin (Herv´e Pageon, 2021). Beside the photoaging, both UVB and UVA have been shown to induce skin cancer like melanoma, which is the most serious type of skin cancer. This type of cancer develops in the melanocytes cells that produce two types of melanin: eumelanin and pheomelanin.

Eumelanin is the most common type in dark skin and dark hair, which reduces the accumulation of UV-induced photoproducts, while pheomelanin may actually contribute to UV-induced DNA damage by inducing free radical formation after UV. So, by limiting the exposure of skin to UVR can help to reduce the risk of melanoma (Ashley Sample, 2018). In addition, the UVR can have other effects on the skin by inducing cellular damage and alterations in immunologic function, gene mutations, immunosuppression, oxidative stress, and inflammatory responses, which all have an important role in skin cancer. For instance, UVA rays can cause skin cells to age and some indirect damage to cells' DNA and they are mainly linked to long-term skin damage such as wrinkles since they reach deeper skin layers. UVB rays damage the DNA in skin cells directly and are the main rays that cause sunburns (Yasuhiro Matsumura, 2003; Deevya L. 2010; Krysta Biniek, 2012), the UV rays penetration into the layers of the skin presence in (**Fig. 3**) (Almudena Pérez-Sánchez, 2018).

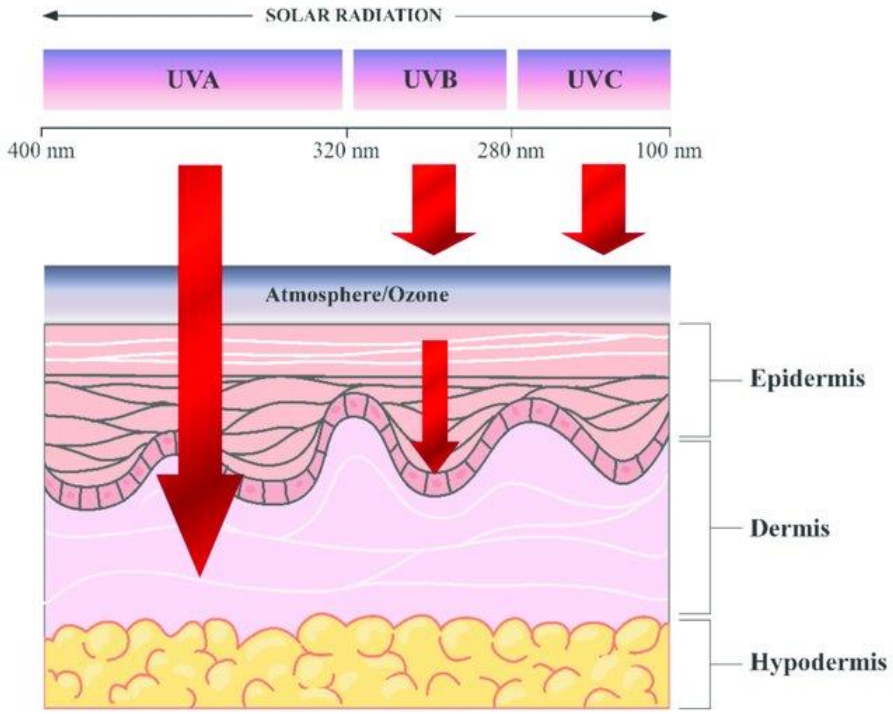

Fig. 3. The UV ray penetration into the layers of the skin.

1.2. Sunscreen Products

Sunscreen is a photoprotective agent for the skin that helps to protect against sunburn and most importantly, prevents the skin cancer like melanoma from the damaging effects of ultraviolet (UV) rays (M.S. LATHA, 2013). Sunscreens can be divided into chemical (organic) filters which absorb UV rays in a certain range of wavelengths and convert it to heat before harmful UV rays penetrate the skin. These filters are further divided into UVB and UVA filters. For instance, UVB filters like: (PABA derivatives, Cinnamates, Salicylates, etc.) and UVA filters like benzophenones, avobenzone, meradimate, etc.).

The other type of filters is the physical (inorganic or mineral) ones, like zinc oxide (ZnO) and titanium dioxide (TiO_2) that reflects/ scatter the UV rays. These types of sunscreen filters, especially zinc oxide, protect the skin against a wide range of specific UVA and UVB rays. But it should be noted that zinc oxide alone is not a suitable sunscreen because the maximum amount allowed to use it in the formulation of sunscreen products is 25%, which only creates an SPF of about 16. On the other hand, physical filters may not be aesthetically acceptable to people due to the change in colour they create on the skin (creating a chalky white colour) (Sowmya Kaimal, 2011). In addition, sunscreens may contain other additives such as antioxidants for decreasing the effect of ROS and DNA damage, since these play an important role in the prevention, improvement, and reduction of free radicals and oxidative stress (Linna L. Guan, 2021).

Sun Protection Factor (SPF):

Sunscreens are characterizing by Sun Protection Factor (SPF), which is a measurement of the protection of the skin from sunburn (Low: SPF 2 – 15; Medium: SPF 15 – 30; High: SPF 30 – 50; Highest: SPF >50). SPF is measured using the following formula:

SPF = MED of protected skin / MED of unprotected skin (MED = minimal erythema dose)

To increase the SPF of sunscreens, it should be used higher amounts of UV filters. Since, the UV filters are fatty and heavy compounds, they increase the secondary reaction in the skin, like sensitivity and acne by blocking the skin pores. Additionally, the amount of the SPF to protect the skin of different people depends on the type and colour of the skin, as well as where the person lives (M.S. LATHA, 2013; Sowmya Kaimal, 2011).

1.3. Environmental Impact of Sunscreens

In today's world, various sunscreens products exist. Over the years, we've seen an influx of sunscreen products in the market from various brands and companies. These range from chemical sunscreens to mineral sunscreens. These products contain various active ultraviolet filter (UVF) ingredients that work to prevent UVA and UVB rays from damaging the skin. Sunscreen manufacturers incorporate UV-absorbing ingredients to reduce UV rays' ability to penetrate the skin. During recreational activities and water sports in natural waters, sunscreen washes off people's skin to disperse in the surrounding environment. Chemical sunscreens are the most commonly used sunscreen and their most common active ingredients – oxybenzone, butylparaben, and octinoxate – which were already identified as environmentally harmful ingredients. Researchers found that the chemicals can have destructive effects on corals, algae, arthropods, molluscs, etc. and generally, these products are a serious threat to marine life. The harmful accumulation of these products in many organisms may be a gateway for their transfer to higher food levels and different ecosystems (Shengwu Yuan, 2022; Myrto Chatzigianni, 2022). Therefore, natural compounds with photoprotective properties have received much attention in recent years because they are safe for the environment and marine, as well as have no side effects on human health.

2. Natural Compounds

As mentioned before, the use of antioxidants in sunscreens is very important like polyphenols.

2.1. Polyphenols

Polyphenols are a group of natural phytochemical compounds that are abundantly found in plant foods such as fruits, vegetables, tea, dark chocolate, and wine, may be an excellent source of antioxidants with UVF properties These compounds can act as an antioxidant and neutralize free radicals that damage body cells and cause cancer and other diseases. Also, by reducing inflammation, they can prevent the occurrence of many chronic diseases (Kanti Bhooshan Pandey, 2009; Haneen Amawi, 2017). So far, more than 8,000 types of polyphenols have been identified, which are divided into different groups according to the number of phenol rings they contain and the structural elements that connect these rings. Polyphenols are mainly classified into 4 main groups: phenolic Acids, flavonoids, lignans, stilbenes. The structures of the family members are highly diverse and complex, which are classified based on the number of phenolic rings and differences in structural elements. Among them, flavonoids are the largest group consisting of about 5000 polyphenols (**Fig. 4**) (Itika Arora, 2019).

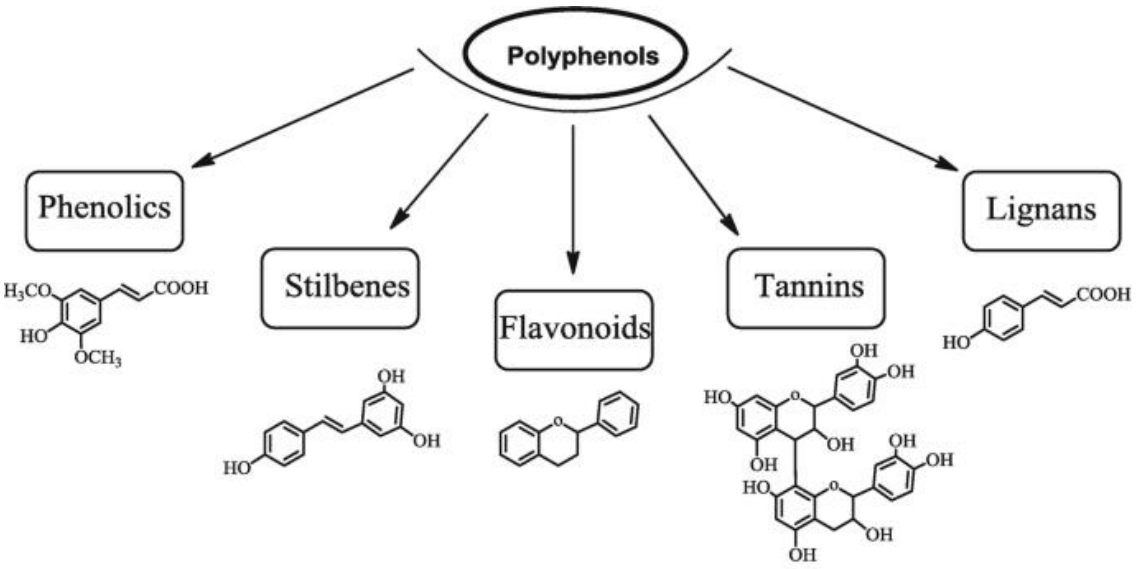

Fig. 4. Classification and chemical structures of the different classes of polyphenols.

2.2. Flavonoids

Flavonoids are a diverse group of plant compounds with two aromatic rings connected by three carbon atoms, forming an oxygenated heterocyclic ring structure, found in several parts of the plant, abundantly found in foods and beverages of plant origin, such as fruits, vegetables, tea, cocoa and wine. Flavonoids have important and various role in biological activities in the plants, since they are the most important plant pigments responsible for colouring fruits, vegetables and flowers with yellow, red, and blue hues, they can also promote the attraction of pollinators, contributing to growth and development of seedlings. Flavonoids can scavenge the ROS, which are produced by the photosynthetic electron transport system and react with nucleic acids, proteins and fatty acids. Furthermore, because of their favourable UV-absorbing properties, flavonoids protect plants from UV radiation of sun and scavenge UV-generated ROS. It has been proved that the flavonoids are one of the most powerful bioactive in protecting the body against reactive oxygen species. Since, human cells are constantly threatened by free radicals and reactive oxygen species, which are produced during normal oxygen metabolism or caused by external damage, flavonoids can be an excellent option for a photo protection (Nisakorn Saewan, 2013; A. N. Panche, 2016). The general structure of flavonoids is a 15-carbon skeleton consisting of 2 benzene rings linked by a 3-carbon linker chain. Different classes of flavonoids differ in the level of oxidation and the substitution pattern of the C ring and they are divided into 6 main groups: (flavones, flavonols, flavanonols, isoflavones, flavan-3-ols, and anthocyanidins) (**Fig. 5**) (Shashank Kumar, 2013).

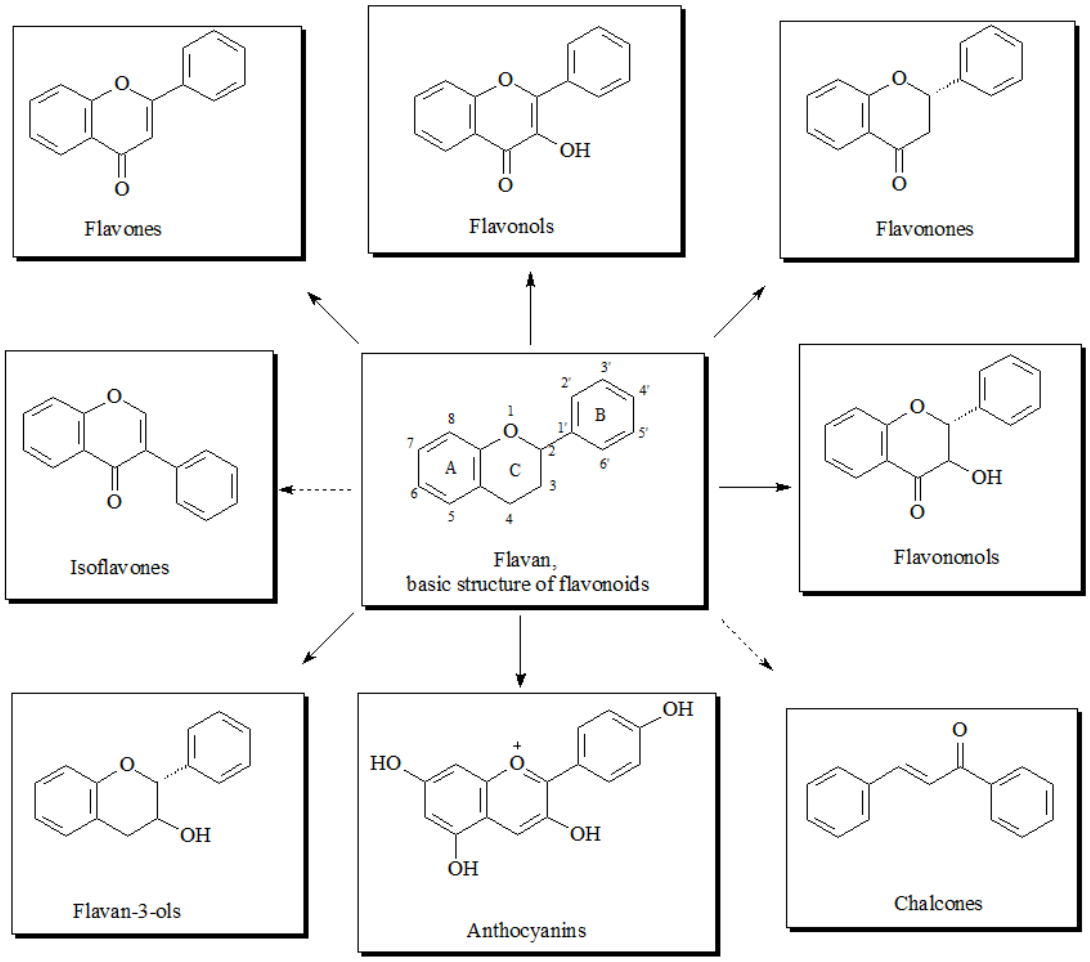

Fig. 5. Basic skeleton structure of flavonoids and their classes.

2.3. Anthocyanins

Anthocyanins are a group of antioxidants that are considered an important water-soluble group of pigments in nature that are responsible for the red, blue, and purple colours of most flowers and fruits and vegetables like red and black berries, black grapes, eggplant, red onion and black beans and others (Adriana Gadioli Tarone, 2020). Anthocyanin is one of the subclasses of flavonoids, which is in the form of glycoside while anthocyanidin is known as the aglycone. Anthocyanidins are grouped into 3-hydroxyanthocyanidins, 3-deoxyanthocyanidins, and O-methylated anthocyanidins, while anthocyanins are in the forms of anthocyanidin glycosides and acylated anthocyanins.

Anthocyanins consists of an anthocyanidin aglycone and one or more sugar moieties linked to hydroxyl groups 3, 5, 7, with the 3 positions on the C-ring being

dominant. With different types and/or numbers of sugars such as glucose, galactose, xylose and fructose, attached to different positions, it creates diverse structures of anthocyanins. The most common anthocyanidins are cyanidin, delphinidin, pelargonidin, peonidin, petunidin, and malvidin, whose structures can be different in the substitution at 3′ and 5′ positions (**Fig. 6**) (Jun Cheng, 2014). Since anthocyanidins have extremely low stability, they are easily affected by a wide range of parameters such as relative humidity, light, pH, and temperature. Therefore, the colour of the anthocyanin depends on the pH and also by methylation or acylation at the hydroxyl groups on the A and B rings (Bianca Enaru, 2021).

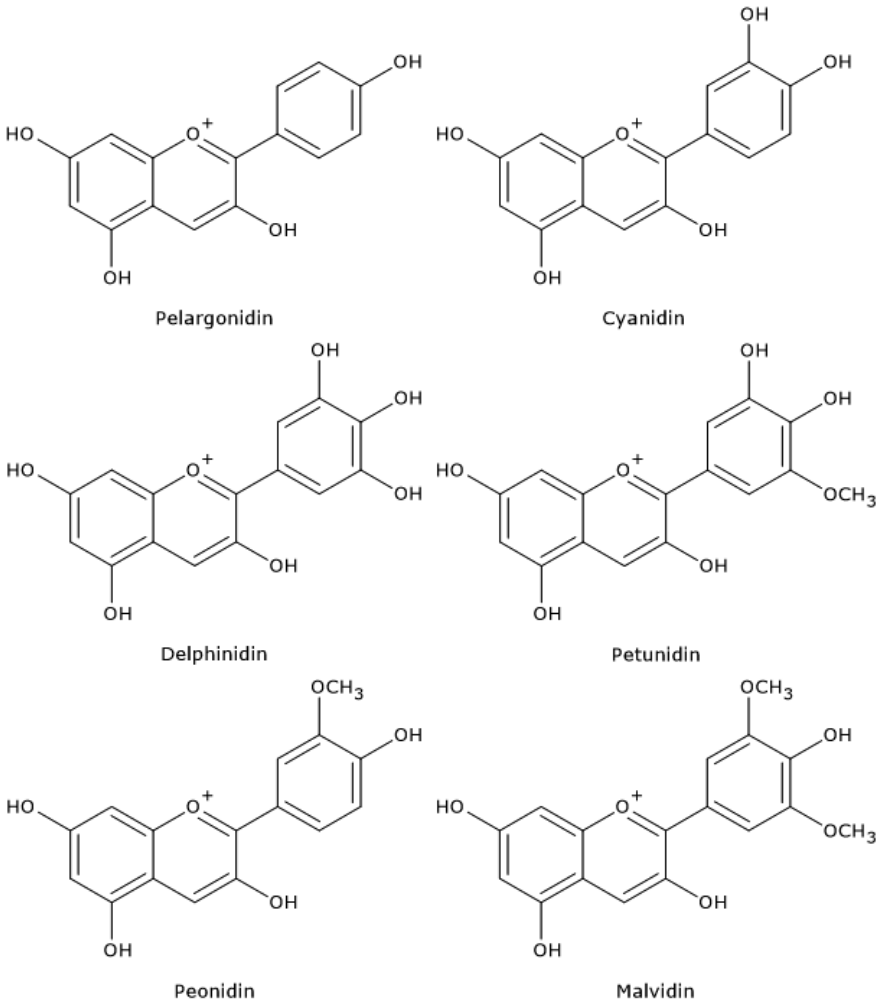

Fig. 6. The structure of the most common anthocyanins present in nature.

Additionally, anthocyanins have several biological properties for protection of skin, such as bacteriostatic, antioxidant and anti-inflammatory effects. Anthocyanins can

act directly as a physical barrier against UV radiation, which exhibit the UV absorption bands in the 280–320 nm range. Beside this, anthocyanins also can reduce the melanoma by influences on abnormal melanogenesis which the cells, responsible to produce melanin. Furthermore, they able to prevent the colonization of microorganisms, such as bacteria, fungi, yeasts, that is this antibacterial behaviour of anthocyanin, beside the high antioxidant properties, increases its importance in a variety of industries (Xusheng Li, 2023). As mentioned, in acidic condition, anthocyanin appears as red-coloured pigment which are predominantly in the form of flavylium cations and they are more stable (lower pH) with higher solubility in water, while with the increase in pH, the pigments turn into purple-blue colour pigments, which indicates the alkaline conditions (**Fig. 7**) (Viirj Kan, 2017; Olivier Dangles, 2018).

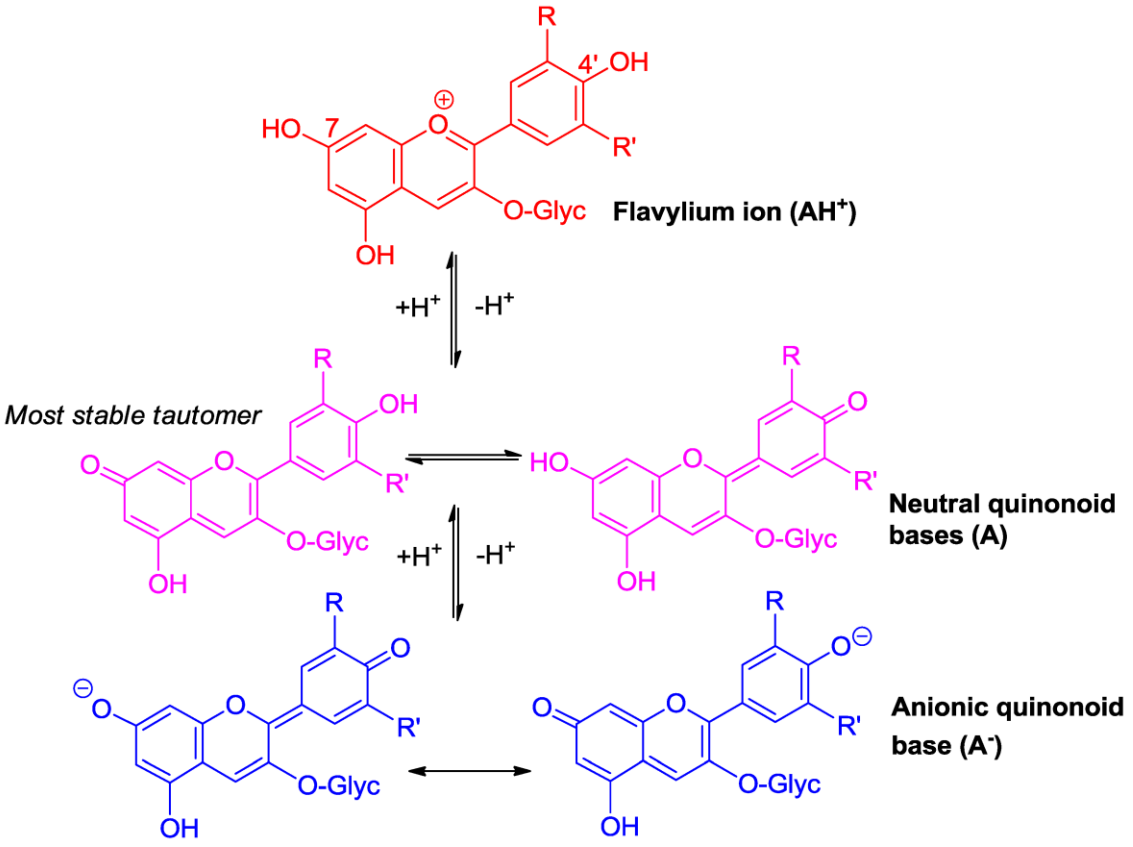

Fig. 7. Chemical diagram of colour-changing anthocyanin pH reaction.

So**,** this is one of the important challenges for scientists to find solutions to increase the stability of anthocyanins in the food ingredients and also cosmetics industry.

Up to now, various methods have been tried to increase the stability of anthocyanins, including co-pigmentation such as combination with caffeine, use of metal ions, but also encapsulation with different polymers (Esra Gençda˘g, 2022).

One such polymer, is lignin which has antioxidant and antimicrobial properties and also have the ability to absorb ultraviolet rays, thus enabling protection against ultraviolet rays. In addition, it has the ability to increase the stability of products, so it has become one of the most widely used ingredients in the cosmetics industry (Viviana S.C. Gagosian, 2022).

2.4. Lignin

Lignin is the second most abundant natural biopolymer after cellulose, which is present in plants often attached to cellulose and hemicellulose forming their main structure (**Fig. 8**) (Mika Henrikki Sipponen, 2019). Lignin is a complex polyphenol, which contains three types of phenyl propane units (Yi Zhang, 2021). Lignin has a non-crystalline structure which is hydrophobic and insoluble in water at acidic or neutral pH. However, lignin can be dissolved in a variety of organic solvents, including ethanol, acetone, and chloroform, as well as in alkali solutions.

In recent years, lignin has been considered as a safer and biodegradable alternative to synthetic UV absorbers in sunscreens, which can contribute to UVB and UVA absorption. However, besides protecting the skin by absorbing sunlight across its whole spectrum, lignin also protects the skin from sunlight by neutralizing ROS that can cause oxidative damage to skin. Since it has high antioxidant property which depend on the substituents of the aromatic ring and side chain structures. It also, can be used as natural preservative in sunscreens by inhibiting the growth of harmful bacteria. Unlike the chemical ingredients of sunscreen such as filters and preservative that are harmful for environment and human health, lignin is a relatively safe option for both the environment and consumers of sunscreens and SPF cosmetics (Petri Widsten, 2020)

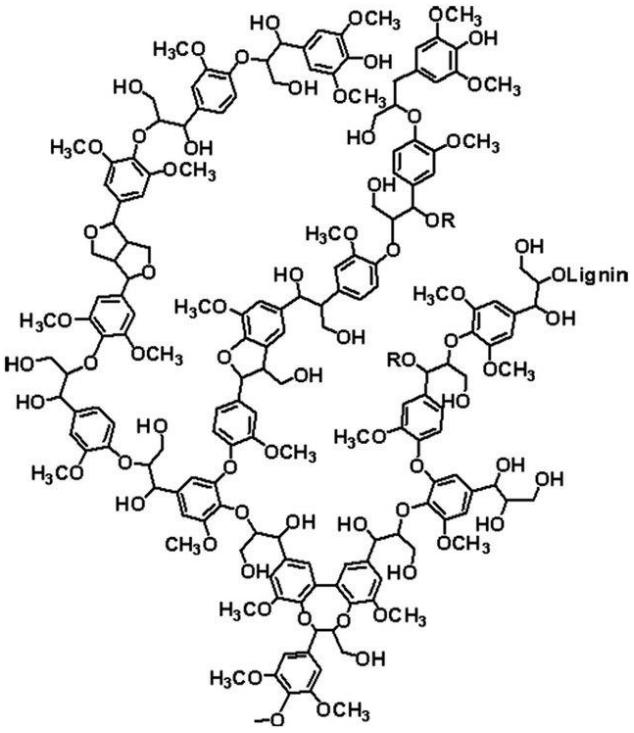

Fig. 8. The chemical structure of Lignin.

2.5. Lignin sulfonate

Lignin has many variations and derivatives, like Lignin sulfonate or sulfonated lignin (**Fig. 9**), which is produced via the sulfite pulping process of the paper and pulp industry. Lignin sulfonates are water-soluble anionic polyelectrolyte polymers that have a hydrophilic end such as sulfonic, phenolic hydroxyl, and alcoholic hydroxyl, and a hydrophobic end such as carbon bonds. This feature causes its high surface activity and it use as a surfactant and stabilizer, which is soluble in water and also have good solubility in ethylene glycol, propylene glycol, dimethyl sulfoxide (DMSO), methanol-water, unlike the organic solvents that are insoluble. Moreover, these types of lignins are usually cross-linked lignins and their average molecular weight is higher than kraft lignin (KL), which is the most abundant aromatic renewable biopolymer that isolated from the kraft pulping processes, which involves wood chip digestion at an elevated temperature (~170 °C) and pressure in an aqueous solution of sodium sulfide and sodium hydroxide (Filipa M. Casimiro, 2022; Jun Liu, 2022; Luis Alberto Zevallos Torres, 2019).

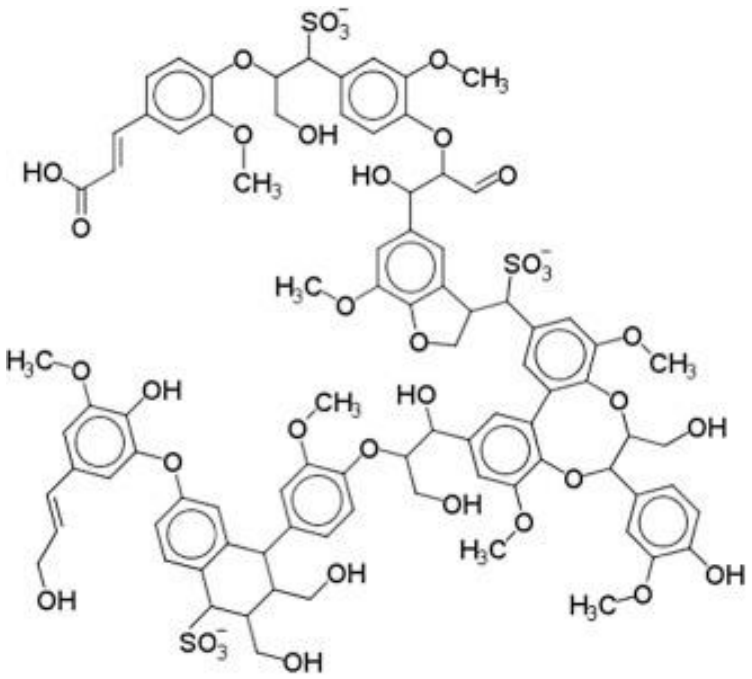

Fig. 9. The chemical structure of Lignin sulfonate.

Goal

This project aims to use Agro-food recycled bioactive compounds including anthocyanins and lignins, to include in innovative applications as skincare ingredients. These bioactives were selected based on their UV protection properties and additional moisturizing, anti-dark spots, anti-wrinkles and wound-healing effects, associated with interesting colours (ranging from red to blue) depending on the composition of the formulation.

Materials and Methods

Materials

RP-18 gel (40-63 μm) LiChroprep, methanol, acetonitrile, formic acid, dimethyl sulfoxide (DMSO), sodium hydroxide (≥98.0%), was purchased from Merck (Darmstadt, Germany), Kraft lignin (MW∼5000 Da) was provided by StoraEnso (Finland).

All the other materials were acquired in companies mention between brackets: aneuploid immortal keratinocytes from adult human skin, (HaCaT, Cell Lines Service, CLS), Dulbecco's Modified Eagle Culture Media (DMEM, CLS), fetal bovine serum (FBS, from Biowest), antibiotic/antimycotic solution (100 units/mL of penicillin, 10 mg/mL of streptomycin and 0.25 mg/mL of amphotericin B, Sigma-Aldrich, St. Louis, MO, USA), 2,2-diphenyl-1-picrylhydrazyl (DPPH), Trolox (6-hydroxy-2,5,7,8-tetramethylchroman-2-carboxylic acid), Carbopol® 974P NF (Carbomer), Geogard® 221 (Benzyl Alcohol), Sodium hydroxide, Tegosoft® TN (C12-15 Alkyl Benzoate), Glycerine, SEPIPLUS™ 400 (Polyacrylate-13), ESAY NOV™ (Octyldodecanol), Tegosoft® TN (C12-15 Alkyl Benzoate), Neo Heliopan® AP (Disodium Phenyl Dibenzimidazole Tetrasulfonate).

Vegetal material: blackberry fruit was graciously provided by Prof. Pedro Oliveira from INIAV, lignosulfonates were prepared and kindly provided by Dra. Carina from FEUP (the original liquor was provided by GRATKRN Company).

Methods

4.1. Extraction of Anthocyanins

In this work, anthocyanins were extracted and purified from blackberry fruit. Extracted anthocyanins were prepared using frozen blackberry (1 Kg) mixed in deionized water (2 Liter) acidified with HCl (0.1 M) under constant stirring (300 rpm) for 2 h at room temperature. After 2h, a second extraction was performed with deionized water (5 Liter) acidified with HCl (0.1 M) under constant stirring (300 rpm) for 24 h at room temperature. The obtained solution was filtered and centrifuged at 14000 rpm during 5 min to remove the fine solids. The supernatant was collected and stored at 4ºC.

4.2. Purification and Identification of Anthocyanins

The aqueous phase of blackberry extract, was applied to a Büchner funnel containing C18 reverse phase gel (Lichroprep, RP-18, Merck™); to remove sugar and other compounds. In order to prevent the degradation of nonacylated anthocyanins and to keep the extracted anthocyanins in a stable form, pH of the extraction medium was kept mildly acidic using HCl 2% (v/v). The extraction was carried out using aqueous methanol with 10% (v/v). Collected fractions were evaporated under vacuum, in a rotary evaporator (Buchi Rotary Evaporator) at 38ºC to remove methanol and to concentrate the anthocyanin extracts. The obtained concentrated extract was kept at -18ºC until it was completely frozen and ready to be placed in the freeze dryer (BenchTop Pro with Omnitroics™). The water was sublimated in vacuum conditions at low temperature (-84.0°C). Accordingly, the liquid extract turns into powder form.

Identification of anthocyanins was performed by uHPLC on a Dionex Ultimate 3000 (Thermo Scientfic) equipped with a 250×4.6mm i.d., 5 µm LicroCART® reversed-phase C18 column (Merck™); detection was carried out at 520 nm using a diode array detector. The solvents were (A) 1% (v/v) HCOOH and (B) 1% (v/v) HCOOH and 30% (v/v) CH_3CN. The gradient consisted of 80–20% A for 90 min, at a flow rate of 1.0 mL/min.

4.3. Preparation of Lignin Nanoparticles

Lignin nanoparticles (LNP) were prepared using nanoprecipitation method, in two different approaches. In the first one, the mix of Kraft lignin (20 mg/mL) and Cy3glc (1.5 mg/ml) was dissolved in 90% (v/v) acetone (1 mL) and the solution was added rapidly to Milli-Q water (1:10) under constant stirring (300 rpm) using a micropipette (20–200 µL). After this step, the solution was kept under continuous stirring during 3 h at room temperature to ensure the acetone evaporation.

In the second one, Kraft lignin (20 mg/mL) dissolved in 90% (v/v) acetone (1 mL) was added rapidly to the mix of Cy3glc (1.5 mg/ml) and Milli-Q water (1:10) under constant stirring (300 rpm) using a micropipette (20–200 µL) After that, the solution was kept under continuous stirring during 3 h at room temperature to ensure the acetone evaporation. In both methods, NPs were prepared in triplicate.

4.3.1. Characterization of Nanoparticles

LNP, obtained by nanoprecipitation were characterized in terms of their average particle size (Z-average) and polydispersity index (PDI) by dynamic light scattering (DLS) and the average zeta (ζ)-potential was determined using electrophoretic light scattering (ELS) in a Malvern Zetasizer Nano ZS instrument (Malvern Instruments Ltd, UK). For these measurements, the samples were diluted 167 times with MilliQ-water and analyzed in triplicate.

4.3.2. Encapsulation Efficiency (EE)

The encapsulation efficiency of the Cy3glc in the lignin nanoparticles was determined by an indirect methodology. For that, 5 mL of both methods solutions were centrifuged at 14000 rpm during 5 min. Then, the concentration of samples on the supernatant was determined by uHPLC on a Dionex Ultimate 3000 (Thermo Scientfic) equipped with a 250×4.6mm i.d., 5 µm LicroCART® reversed-phase C18 column (Merck™); detection was carried out at 520 nm using a diode array detector. The solvents were (A) 1% (v/v) HCOOH and (B) 1% (v/v) HCOOH and 30% (v/v) CH_3CN. The gradient consisted of 80–20% A for 90 min, at a flow rate of 1.0 mL/min.

The encapsulation efficiency (EE) was determined through the following equation:

$$EE\ (\%) = \frac{(\text{Total concentration of pigment} - \text{Free pigment concentration})}{\text{Total concentration of pigment}} \times 100$$

4.4. Anthocyanin Stability in Different Storage Conditions (interaction with lignosulfonates)

To determine the colour stability over time of Cy3glc in the presence or absence of lignosulfonates, the UV-Vis spectra of samples, free Cy3glc, free LS and mixture of both were prepared at 0.4 mg/mL concentration in Milli-Q water at four different pHs (pH 3, pH 4, pH 4.5, pH 5). The spectrum at zero time was measured in (FlexStation 3 Multi-Mode Microplate Reader (Molecular Devices)), in the range between 350-750 nm wavelength, and splitted the samples to three different conditions (dark, light, 40°C). After 30 days, the spectrum was measured again in the same wavelength range.

4.5. Cell Culture Assays

4.5.1. Cell Lines and Growth Conditions

Aneuploid immortal keratinocytes from adult human skin, (HaCaT, Cell Lines Service, CLS) were cultured in T75 flasks and maintained Dulbecco's Modified Eagle Medium (DMEM, CLS) supplemented with 10 % fetal bovine serum (FBS, from Biowest) and 1 % of antibiotic/antimycotic solution (100 units/mL of penicillin, 10 mg/mL of

streptomycin and 0.25 mg/mL of amphotericin B, Sigma-Aldrich, St. Louis, MO, USA), at 37 ºC in an atmosphere of 5 % CO2. Medium was renewed every two days and cells were harvested when necessary.

4.5.2. Cytotoxicity Evaluation

For the toxicity evaluation, HaCat cells were seeded in 96 well plates at a density of 4×10^5 cells/mL and left to attach for 24h to reach a state of confluent cell layers. Serially diluted compound solutions of lignosulfonates and cyanidin-3-glucoside were prepared in DMEM and added to the wells. After an incubation period of 48 h at 37 ºC, cellular viability was determined by MTT assay. Briefly, an MTT solution prepared in DMEM (0.2 mg/mL) was added to each well (100 µL). After 30 min of incubation, the medium was removed and formazan crystals were dissolved in dimethylsulfoxide (DMSO, Sigma-Aldrich). Absorbance was read at 570 nm in a FlexStation 3 Multi-Mode Microplate Reader (Molecular Devices). Experiments were performed in triplicates. The percentage of cell viability was determined using the following equation: % cell viability = $A_{sample}/A_{control} \times 100$, where A_{sample} represents the absorbance of wells treated with the compounds at a given concentration and $A_{control}$ corresponds to absorbance of control wells, where cells were not subjected to treatment. Data are expressed as mean absorbance ± standard error of the mean.

$$Cell\ Viability\ \% = \frac{Absorbance\ of\ sample}{Absorbance\ of\ control} \times 100$$

4.6. Radical Scavenging Activity (DPPH assay)

The free radical scavenging activity of the different samples described in (**Table. 2**), was measured in vitro by 2,2-diphenyl-1-picrylhydrazyl (DPPH) assay. A total of 1.18 mg of DPPH were dissolved in 50 mL of methanol for making the stock solution and kept

in dark, which yielded a usable mixture with an absorbance at 517 nm using the spectrophotometer (FlexStation 3 Multi-Mode Microplate Reader (Molecular Devices)). In test tubes, each samples dissolved in Milli-Q water (0.15 mg/mL) and prepared diluted samples (15, 7.5, 3.75, 1.875, 0.9375, 0.46875, 0.234375 mg/mL concentration) in eppendorf tubes. A 30 µL of samples was mixed with 270 µL of DPPH solution and the mixture incubated in the dark for 30 min at room temperature. Then the absorbance was therefore determined at 517 nm. Also the control was prepared as above without any sample. Results were expressed in Trolox equivalents. The following formula was used to compute the percentage of antioxidants:

$$\%\ \text{of antioxidant activity} = \frac{(\text{Control reaction absorbance} - \text{Testing specimen absorbance})}{\text{Control reaction absorbance}} \times 100$$

Table. 2. Different samples using in DPPH Assay.

Samples	Amounts (mg)	Solvent (Milli-Q water) (mL)
Trolox	1	6.7
LS	1	6.7
Cy3glc	1	6.7
Blackberry Extract	1	6.7
Cy3glc + LS	1 + 1	6.7
Cy3glc + LS	1 + 4.5	6.7

4.6.1. Calculation of Trolox Equivalent Antioxidant Capacity

The DPPH radical scavenging activity of sample was expressed as Trolox equivalent antioxidant capacity (TEAC). TEAC was calculated as follows:

$$TEAC = \frac{IC_{50}\ of\ Trolox\ (\mu g/ml)}{IC_{50}\ of\ Sample\ (\mu g/ml)}$$

Where the IC_{50} (inhibitory concentration-50) is the concentration of an antioxidant-containing substance required to scavenge 50% of the initial DPPH radicals. The lower the IC_{50} value, the more potent is the substance at scavenging DPPH and this implies a higher antioxidant activity.

4.7. Determination of Solar Protection Factor (SPF)

To determine the in vitro solar protection factor (SPF), a relative measure of UVB protection, 1.0 mg of each compound/extract was weighed, transferred to a 5 mL volumetric flask, diluted to volume with Milli-Q water water (pH 4.5), followed by ultra-sonication for 5 min. The absorption spectrum of each sample was collected in the range of 290 to 320 nm (every 5 nm) and with 3 measurements for each point, using a 1 mm quartz cell and water (pH 4.5) as a blank. SPF values were calculated according to Mansur equation, Where CF (correction factor) is 10, EE (λ) represents the erythmogenic effect of radiation with wavelength λ, Abs refers to spectrophotometric absorbance values at each wavelength λ. EE(λ) × I(λ) values are constant and are presented in (**Table. 3**).

Table. 3. Normalized product function used for the calculation of SPF.

λ (nm)	EE x I (normalized)
290	0.0150
295	0.0817
300	0.2874
305	0.3278
310	0.1864
315	0.0839
320	0.0180
Total	1

EE – erythemal effect spectrum; I – solar intensity spectrum

$$SPF_{\text{spectrophotometric}} = CF \times \sum_{290}^{320} EE\ (\lambda) \times I\ (\lambda) \times Abs\ (\lambda)$$

4.8. Formulation

Two different formulations were developed, based on structure and ingredients (**Table. 4, 5**), appearance, viscosity and physical stability.

4.8.1. Preparation of Gel Serum

Anthocyanin (blackberry extract) and lignosulfonates were first solubilized in the aqueous part of the serum, containing water, glycerin and the preservative. In the case of the nanoparticles, since they are dispersing in an aqueous solution, instead of powder form, the corresponding water volume was subtracted from the total volume of aqueous fraction. After complete solubilisation of the natural ingredients, the polymer Carbopol® 974P NF added and gently mixed. After obtaining a homogeneous jellified structure, Tegosoft GC was gradually added. A neutralization step was then required to achieve maximum viscosity. In the case of this type of polymers once a neutralizer is added to the dispersion, thickening gradually occurs. In the formulation step, NaOH was selected as neutralizer to achieve the desired thickening effect (**Fig. 10**). All procedure of raw material incorporation and mixing was conducted manually at room temperature. Then the gel serums were splitted into three different conditions (dark, light, 40°C).

Table. 4. Ingredients of Gel Serum.

Ingredient	INCI	% (m/m)
Purified water	Aqua	Qb/100
Carbopol® 974P NF	Carbomer	0.5
Geogard® 221	Benzyl Alcohol	0.5
NaOH 10 M	Sodium hydroxide	Qb/pH 5-6
Tegosoft® TN	C12-15 Alkyl Benzoate	3
Glycerine	Glycerine	10

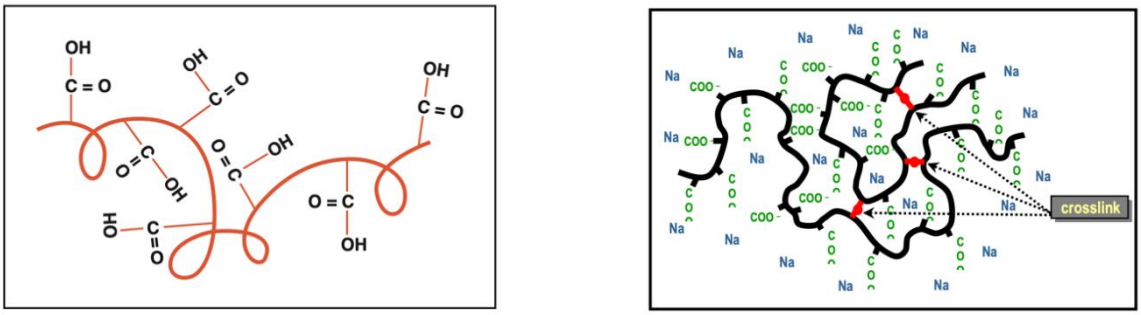

a) b)

Fig. 10. a) The structure of Carbopol® 974P NF polymer; b) The structure of Carbopol® 974P NF polymer after adding NaOH 10 M.

4.8.2. Preparation of Gel-in-oil Emulsion (GELTRAP)

The principle of obtaining GELTRAP emulsion was to gently envelope a gelled aqueous internal phase in a lipid film. Primary the ingredients of aqueous phase (**Table. 5**), which are 3% (m/m) SEPIPLUS 400 and 1% (m/m) Geogard 221, are mixed in water, then this phase was slowly stirred until it was completely homogenized as jellified structure. In the next step, the ingredients of oil phase, which are 3% (m/m) ESAYNOV with 2% (m/m) Tegosoft TN were added to prepared gel phase and gently stirred until it was completely homogenized phase as a cream-like phase for 5-10 minutes while the oil phase must envelop the gel phase completely. The obtained emulsion leaved for 24 hours at room temperature in the dark to rest. The GELTRAP emulsions were splitted to three different conditions (dark, light, 40°C).

Table. 5. Ingredients of Gel-in-oil Emulsion.

Ingredient	INCI	% (m/m)
Purified water	Aqua	Qb/100
SEPIPLUS™ 400	Polyacrylate-13	3
Geogard® 221	Benzyl Alcohol	1
ESAY NOV™	Octyldodecanol	3
Tegosoft® TN	C12-15 Alkyl Benzoate	2
Neo Heliopan® AP	Disodium Phenyl Dibenzimidazole Tetrasulfonate	3

4.8.3. Rheological Behaviour Analysis

The rheological properties were assessed on a rotational rheometer (Kinexus lab+, Malvern, Worcestershire, United Kingdom) equipped with a geometry of parallel plates, one of which rotates (20 mm, 60 mm with a gap of 1 mm) based on a rotational test to measuring the viscosity and elasticity of non-Newtonian fluids under a wide range of conditions and establishing an interrelation between deformation, force and time. The analysis was performed at 25 °C in a shear rate range from 0.1 to 100 s^{-1}, for two series of samples. Data were collected using the rSpace software® (Kinexus 1,75: PSS0211-17). The final results were represented in a graph that relates the apparent viscosity, expressed as Pa.s, and the shear rate, expressed as s^{-1}.

4.8.4. Colour Measurements

Serum series of samples were measured manually, the photos were taken by cell phone with the same light at the same condition and the software in the computer was used to recorded the value of the colours. Cream series of samples were measured by TRA 520 Handheld Benchtop Sphere Spectrophotometer (Lovibond, UK), with CIELab measurements, D65, 10º method in 3x1 cm glass cells. 5 mL of each sample was filled in the cells and the values were recorded by equipment, which the raw values (L, a, b) were calculated by the equation of delta E:

$$\Delta E^*_{ab} = \sqrt{(L^*_2 - L^*_1)^2 + (a^*_2 - a^*_1)^2 + (b^*_2 - b^*_1)^2}$$

Results and Discussion

5.1. Characterization of Extracts by HPLC and Purification of the Anthocyanins

Blackberry anthocyanin extract was analyzed by uHPLC, (**Fig. 11**) shows the chromatogram obtained for the blackberry anthocyanin extract at λ = 520 nm and λ = 280 nm. In the chromatogram it is possible to identify the presence of Cyanidin-3-O-glucoside in both samples. Using the total area of the peaks present in the chromatograms obtained and the calibration curve, the total concentration of anthocyanins present in the extract was determined, resulting in a concentration of (0.123 ± 0.01) mg of anthocyanins (in equivalents of Cy3glc) per mg of extract. Using mass spectrometry, 4 anthocyanins were identified in the 100% methanol fraction, namely: peak 1 - Cyanidin-3-O-glucoside; peak 2 - Cyanidin-3-O-galactoside; peak 3 - Cyanidin-3-O-rutinoside; and peak 4 - Cyanidin-3-O-xyloside, whose characteristics are shown in (**Table. 6**).

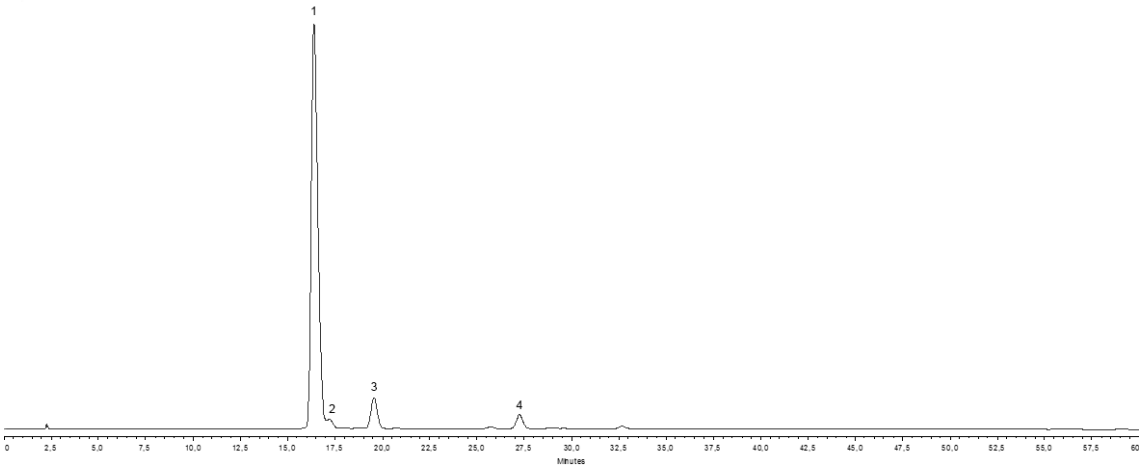

Fig. 11. Chromatogram of HPLC analysis of anthocyanins present in blackberry extract at λ = 520 nm, peak 1- Cyanidin-3-O-glucoside; peak 2- Cyanidin-3-O-galactoside; peak 3- Cyanidin-3-O-rutinoside and peak 4- Cyanidin-3-O-xyloside.

Table. 6. Identification of anthocyanins present in blackberry extract at λ = 520 nm.

Peak	*RT (min)*	*MS*^{1} (m/z)	*MS*^{2} (m/z)	*λ (nm)*	*Anthocyanins*
1	16.57	449	287	502	Cyanidin-3-O-glucoside
2	17.31	449	287	514	Cyanidin-3-O-galactoside
3	19.53	595	449/287	517	Cyanidin-3-O-rutinoside
4	27.45	419	287	517	Cyanidin-3-O-xyloside

With the aim to obtain pure compound (Cyanidin-3-*O*-glucoside) free from any impurities, including other classes of phenolic compounds, and other anthocyanins, the total anthocyanin blackberry extract was applied in low pressure C18 silica gel. As can be observed in the chromatogram of (**Fig. 12**), Cyanidin-3-*O*-glucoside was purified at a percentage of 92% (**Table. 7**), which was obtained by the sum of all available peaks present in the chromatograms divided by the area of the main peak (Cy3glc) and multiplied by 100, whereas, the extract was purified at a percentage of 84%. This means, we able to obtain a pure compound free from impurities. The chemical structures of the identified compounds are represented in (**Fig. 13**).

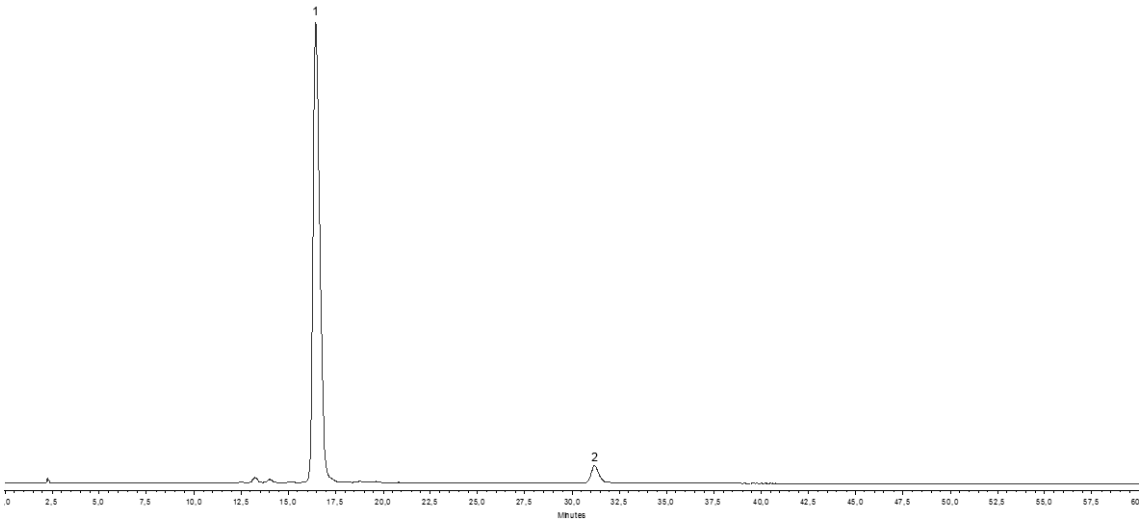

Fig. 12. Chromatogram of HPLC analysis of 10% methanol fraction of anthocyanins present in blackberry extract at λ = 520 nm.

Table. 7. Structural identification of 10% methanol fraction of anthocyanins present in blackberry extract at λ = 520 nm.

Peak	*RT (min)*	*MS*^{1} (m/z)	*MS*^{2} (m/z)	*λ (nm)*	*Anthocyanins*
1	16.57	449.16	287.07	502	Cyanidin-3-O-glucoside
2	31.35	453.36	435.38	292,480	Unknown

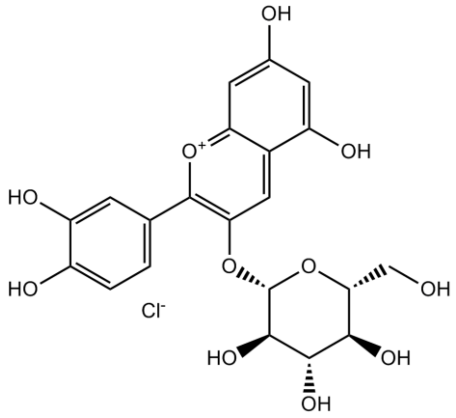

Fig. 13. The chemical structure of the identified compound which was Cyanidin-3-O-glucoside.

The chromatogram obtained for the blackberry anthocyanin extract at λ = 280 nm, is shown in (**Fig. 14**). Through the chromatogram of the extract it is possible to identify the presence of: 1, 2 and 3 - Unknown; 4 - Cyanidin-3-O-glucoside; 5 – Cyanidin-3-O-galactoside; 6 - Cyanidin-3-O-rutinoside; 7 - Cyanidin-3-O-xyloside; and 8 - Unknown, whose characteristics are shown in (**Table. 8**).

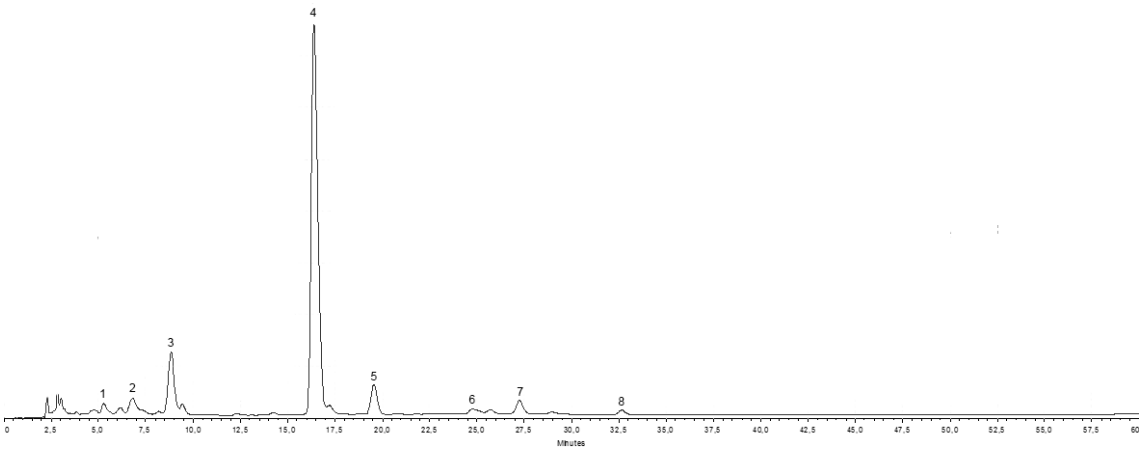

Fig. 14. Chromatogram of HPLC analysis of low molecular weight anthocyanins present in blackberry extract at λ = 280 nm.

Table. 8. Structural identification of low molecular weight anthocyanins present in blackberry extract at λ = 280 nm.

Peak	*RT (min)*	*MS[1]* (m/z)	*MS[2]* (m/z)	*λ (nm)*	*Anthocyanins*
1	5.33	227.15	209.11		Unknown
2	6.82	227.15	209.11		Unknown
3	8.93	249	-	295	Unknown
4	16.57	449.16	361.15	490	Cyanidin-3-O-glucoside
5	17.31	449	287	514	Cyanidin-3-O-galactoside
6	19.53	595	449	517	Cyanidin-3-O-rutinoside
7	27.45	419	287	517	Cyanidin-3-O-xyloside
8	32.69	453.36	435.28	292; 480	Unknown

Also, the chromatogram obtained for 10% methanol fraction of anthocyanins present in blackberry extract at the λ = 280 nm, using the low molecular weight, is shown in (**Fig. 15**). Through the chromatogram of the extract it is possible to identify the presence of: 1 - Unknown; 2 - Cyanidin-3-O-glucoside; 3 - Cyanidin-3-O-galactoside, whose characteristics are shown in (**Table. 9**).

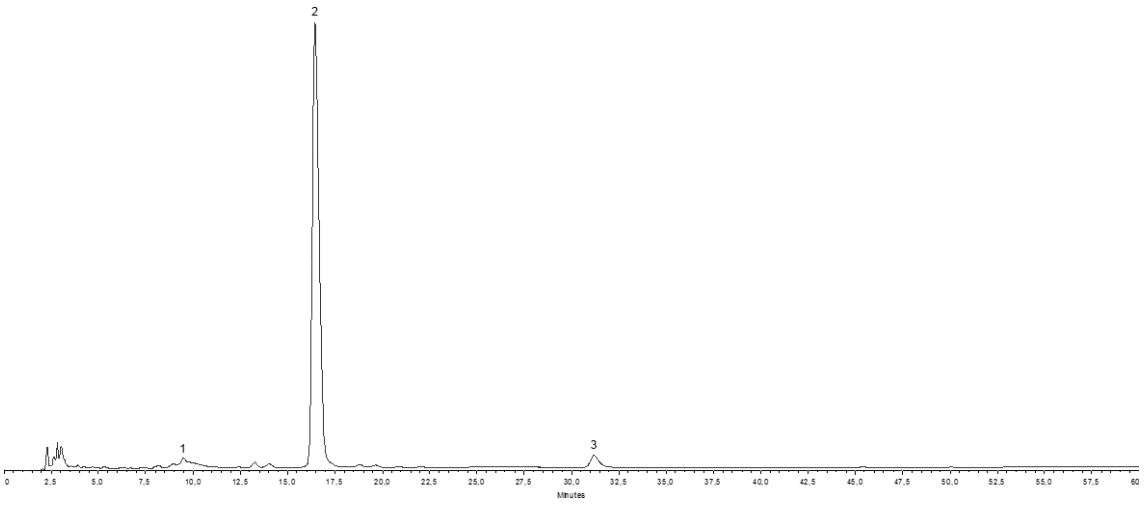

Fig. 15. Chromatogram of HPLC analysis of blackberry extract at λ = 280 nm, after purification in C18 silica gel.

Table. 9. Structural identification of low molecular weight anthocyanins present in blackberry extract at λ = 280 nm, after purification in C18 silica gel.

Peak	*RT (min)*	*MS*^{1} (m/z)	*MS*^{2} (m/z)	*λ (nm)*	*Anthocyanins*
1	9.51	249	-	295	Unknown
2	16.57	449.16	287.07	502	Cyanidin-3-O-glucoside
3	27.45	419	287	517	Cyanidin-3-O-xyloside

Overall, we were able to obtain the pure compound (Cyanidin-3-O-glucoside), which can protect the skin cells against the adverse effects of UVB radiation and skin damage. Therefore, it can be one of the good options of ingredients for the skin products, such as sunscreens, to increase skin protection against UV rays.

Besides these advantages, we know that anthocyanins are very unstable when exposed to light, temperature, oxygen and basic pHs, nevertheless it is possible to increase their stability by different methods such as copigmentaion with caffeine or encapsulation (Esra Gençda˘g, 2022), which can improve the stability of these compounds. When the compound is encapsulated, the bioactive compounds are protected by the wall materials that form microcapsules, which decrease the molar amount of other equilibrium forms, secondary intermediates or degradation products (Loredana Dumitras, cu, 2021).

5.2. Characterization of Nanoparticles

As mentioned, to increase the stability of Cy3glc, the nanoprecipitation method was used. The ability of Kraft lignin, which is the most abundant aromatic renewable biopolymer, for the entrapment of the water soluble red pigment of Cy3glc was evaluated. The obtained nanoparticles were characterized with dynamic light scattering (DLS) and electrophoretic light scattering (ELS) by measuring their average particle size (Z-

average), polydispersity index (PDI) and average zeta potential (ζ) and the results obtained are presented in (**Fig. 16**).

By using the nanoprecipitation method, LNPs presented an average size of (129 ± 9.16 nm) (**Fig. 16a**) and a polydispersity index around (0.2 ± 0.03) (**Fig. 16b**). In contrast, LNP/Cy3glc+H_2O displayed higher particle sizes (226 ± 32.6 nm) (**Fig. 16a**) and polydispersity index (0.5 ± 0.03) (**Fig. 16b**). On the other hand, L, Cy3glc NPs presented an average size of (155 ± 10.63 nm) (**Fig. 16a**) and a polydispersity index around (0.2 ± 0.01) (**Fig. 16b**). Concerning the average zeta potential (ζ), it was observed that as well as the size and polydispersity of LNPs and L, Cy3glc NPs, the values of zeta potential (ζ) were statistically similar and around – 40 mV (**Fig. 16c**) that indicates the presence of a negative charge on the surface of the particles causing repulsion between the particles, which is important for their stability. While, the value of zeta potential (ζ) of LNP/Cy3glc+H_2O was around – 28 mV.

In consequence, after observing all the obtained results, it was clear that the nanoprecipitation method in LNP/Cy3glc+H_2O way had quite different results in compared with LNPs results. In the other hand, L, Cy3glc NPs way had similar results in compared with LNPs results, which was selected to prepare the nanoparticles for the following assays.

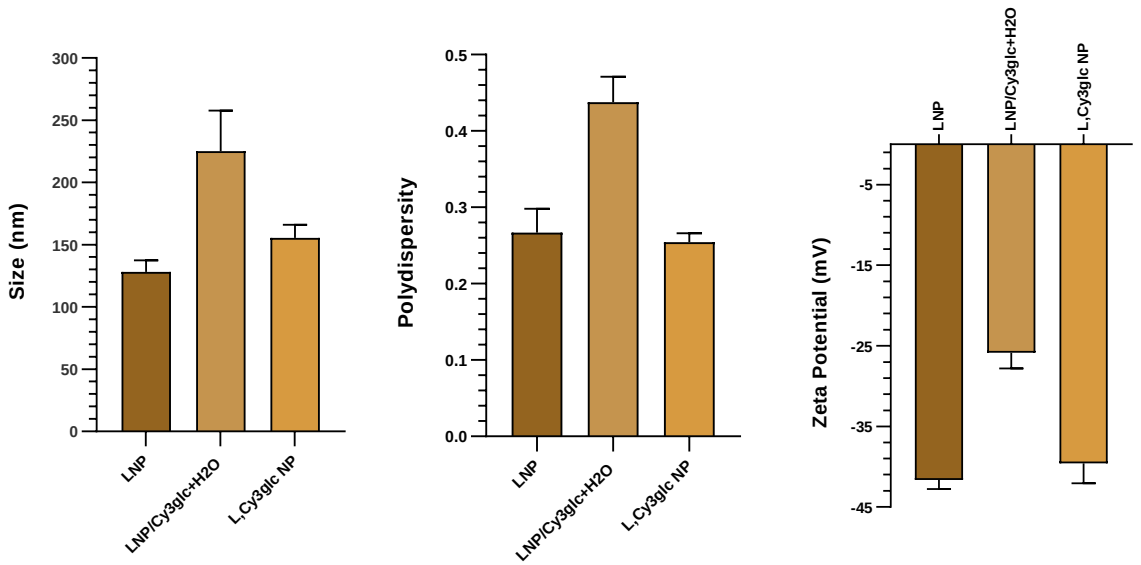

a) b) c)

Fig. 16. Nanoparticles prepared by nanoprecipitation methods (a) - average particle size (Z-average), (b) - polydispersity index (PDI) and (c) - average zeta potential (ζ of LNP, LNP/Cy3glc+H_2O and L, Cy3glc NP. Tukey's multiple comparison test with a 95% significance level using GraphPad Prism 7.04 was used and the level of the significant differences was set at probabilities of a ($p < 0.001$).

5.2.1. Encapsulation Efficiency (EE)

The encapsulation efficiency of the red pigment of the Cy3glc in the lignin nanoparticles was determined indirectly by quantifying the amount of free pigment present in the supernatant by uHPLC. The EE observed for these pigments was 16.55 ± 9.94% and 43.11 ± 1.03% for LNP/Cy3glc+H_2O and L, Cy3glc NPs (**Table. 10**), which in the L, Cy3glc NPs method was higher than the LNP/Cy3glc+H_2O method. This means, the amount of concentration of free Cy3glc in the supernatant in compared with control was low and lignin nanoparticles could capsulated the more Cy3glc than in, Cy3glc NPs method.

Table. 10. Determination of the encapsulation efficiency of the Cy3glc indirectly by uHPLC.

Sample	Free Cy3glc Concentration (mg/mL)(mean ± SD)	Encapsulation Efficiency % (mean ± SD)
Free Cy3glc (Control)	0.123 ± 0.01	-
LNP/Cy3glc+H_2O	0.138 ± 0.02	16.55 ± 9.94
L,Cy3glc NP	0.085 ± 0.02	43.11 ± 1.03

5.3. Anthocyanin Stability in Different Storage Conditions (interaction with lignosulfonates)

Based on the results obtained during 30 days which were collected and are present in (**Fig. 17-18**), lignosulfonates promoted a shift of Cy3glc red colour to more intense red hues at zero time in all different pHs. Obviously, the intensity of the red pigment of Cy3glc with combination of LS, looks darker compared to the free Cy3glc colour and it has preserved the intensity of the red pigments to an acceptable extent, which means that LS interaction with Cy3glc, has been able to increase the stability of Cy3glc. Furthermore, the 30-days results of the graphs also confirm the stability of the combination of LS with Cy3glc, especially in dark condition. Under light conditions, it showed some reduction in red pigment, however, the combination of LS with Cy3glc was still more stable than the free form. As we know, anthocyanin has low stability under light condition, since, light can effect on the synthesis of anthocyanins by influencing photosynthesis and consequently the synthesis of sugar, phenylalanine and other precursor substances (Dongnan Shao, 2022). Therefore, it was expected that the samples would lose their colour under light condition. In other hand, in 40ºC condition, the intensity of the red pigment of Cy3glc with combination of LS, looks darker compared to the free Cy3glc colour and also, both free Cy3glc and combination Cy3glc with LS look darker compared to the under light condition. While, the intensity of the red pigment of free Cy3glc and combination Cy3glc with LS, looks fainter compared to the dark condition especially in 4.5, 5 pHs, which it has been proven that higher temperatures can decrease the stability of anthocyanins by repressing the expression levels of anthocyanin biosynthetic genes, the activity of phenylalanine ammonia-lyase and biosynthetic enzyme (Chikako Honda, 2014).

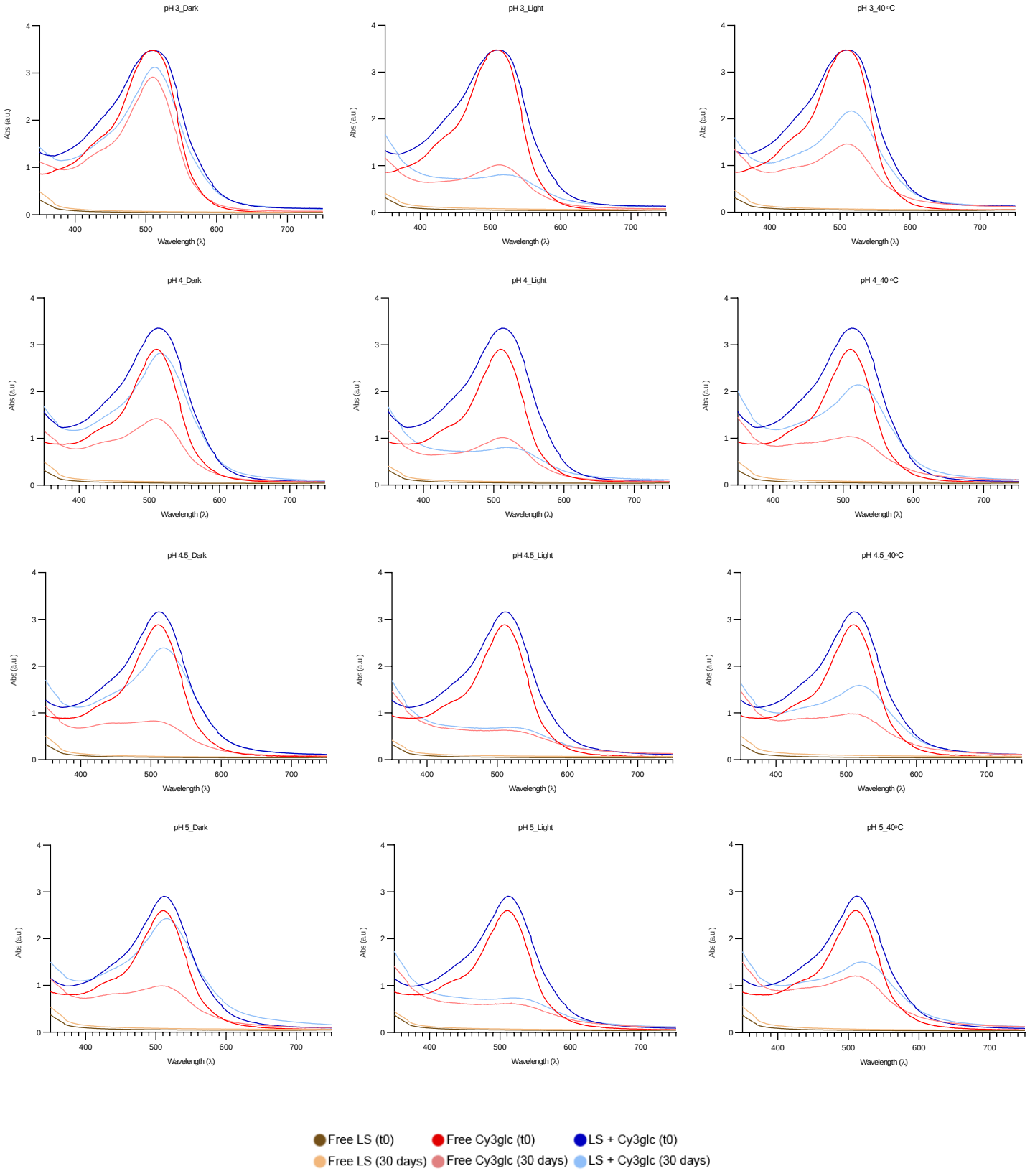

Fig. 17. The results obtained during 30 days based on anthocyanin stability in different storage conditions (dark, light, 40ºC), in different pHs (3, 4, 4.5, 5).

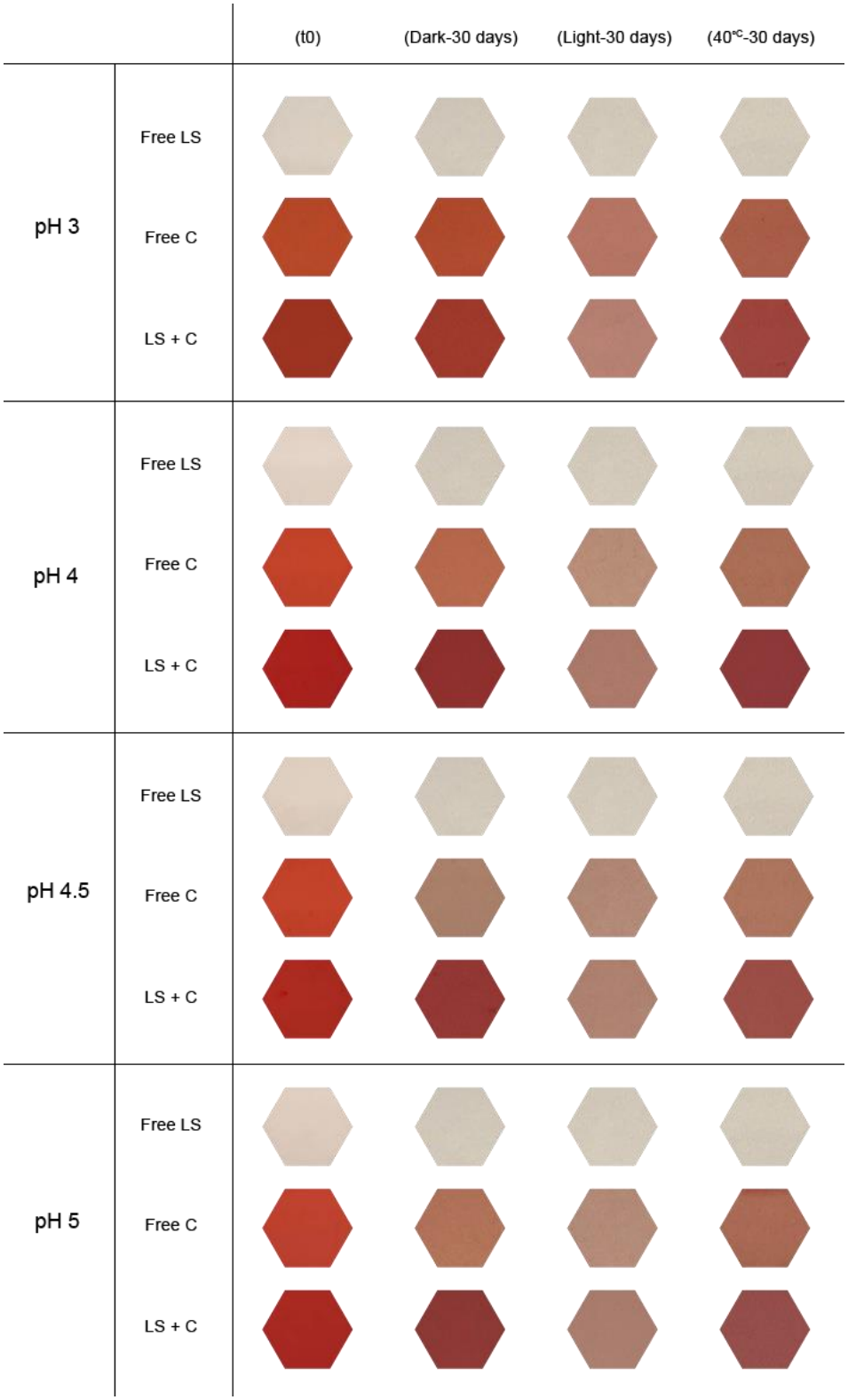

Fig. 18. The colours of samples obtained during 30 days based on anthocyanin stability in different storage conditions (dark, light, 40ºC), in different pHs (3, 4, 4.5, 5).

5.4. Cell Culture Assays

Cytotoxic effects towards human epidermal keratinocytes evaluated by MTT assay. According to the results obtained, over a period of 48 h of incubation, Cy3glc and lignosulfonates (LS) had no significant cytotoxicity towards this cell line at concentrations below 2 and 0.5 mg/mL for LS and Cy3glc respectively, (**Fig. 19**). Although, the conditions applied are very drastic, these results are indicative that even after 2 days in contact with the skin, both bioactives appeared safe and suitable for potential application in topical formulations.

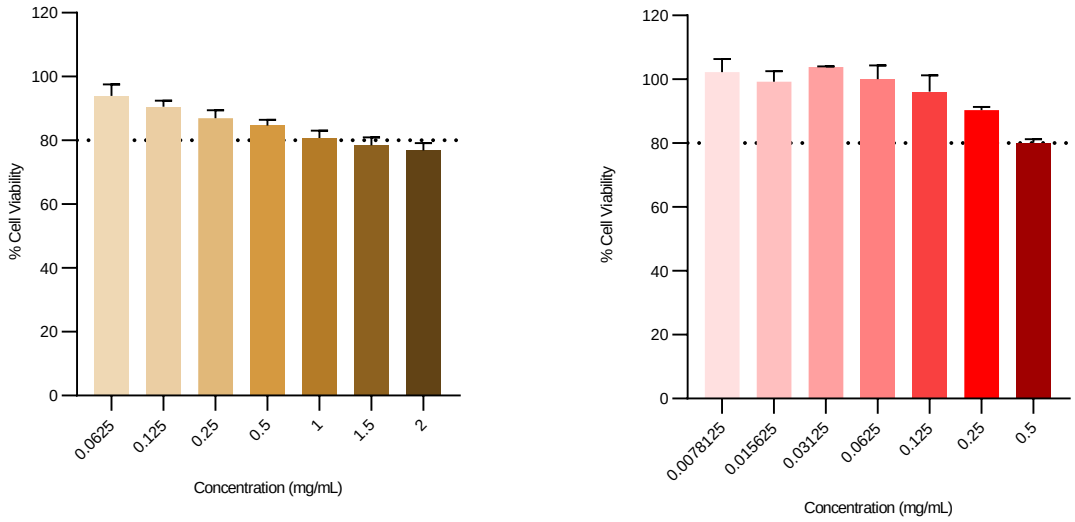

a) b)

Fig. 19. Cell viability of HaCat cell lines in the presence of increasing concentrations of the a) lignosulfonates; b) Cy3glc, evaluated by MTT assay. Dotted lines represent 80% viability.

5.5. Radical Scavenging Activity (DPPH assay)

Antioxidants can help compensate for sunscreen's inherent shortcomings (and for human error in application) by neutralizing the free-radical damage that sun exposure causes. They play a defensive role by diffusing the effects of the bad rays that make it through the sunscreen. Therefore, this property has led to antioxidants being one of the

important ingredients of sunscreens (Ana Jesus, 2023). **Fig. 20.** shows that the scavenging effects of samples on DPPH radical were in the following order: Cy3glc > Cy3glc + LS (1:4.5) > Cy3glc + LS (1:1) > Blackberry Extract > Trolox > Cy3glc + LS (1:1) > LS. Cy3glc and the combination of Cy3glc with LS (4.5 mg) have the highest antioxidant activity. It was expected that the antioxidant activity of the Cy3glc will be high. Since, it has been proven, that anthocyanins can transfer electrons to ROS and thus can protect important oxidizable biomolecules such as unsaturated fatty acids, proteins and DNA, which can be prevent the DNA damage and skin cancer (Olivier O. Dangles, 2020).

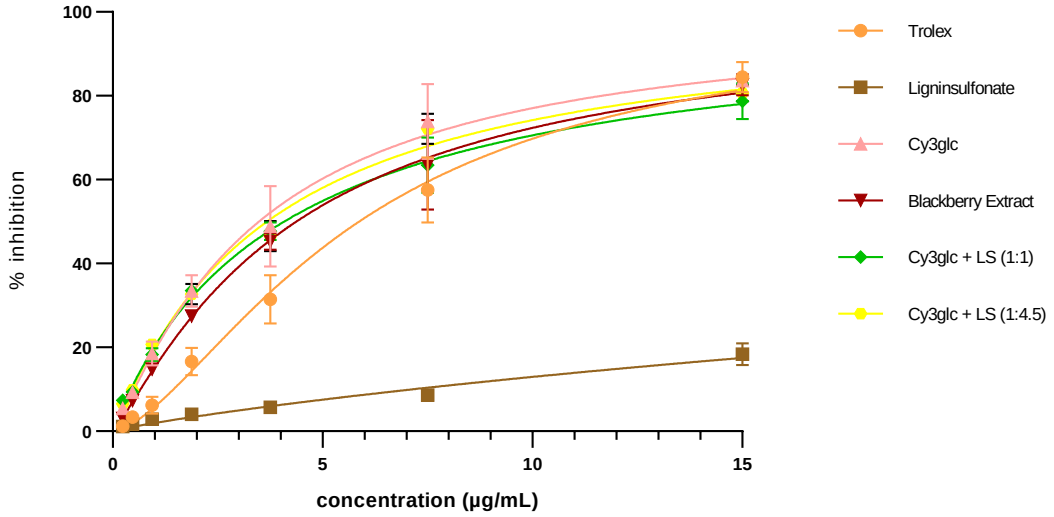

Fig. 20. The percentage of radical scavenging activity of samples with different concentration in presence of Trolox control. Values are the average of triplicate experiments.

5.5.1. Calculation of Trolox Equivalent Antioxidant Capacity

Table. 11. shows the inhibitory concentration (IC_{50} values of the standard (Trolox) and samples. Cy3glc recorded the lowest IC_{50} value of 3.60 µg/mL, followed by Cy3glc + LS (1:4.5) which was 3.86 µg/mL, then Cy3glc + LS (1:1) with a value of 4.17 µg/mL and lastly Blackberry Extract with a value of 5.88 µg/mL. Beside these values of IC_{50}, the TEAC of each sample with respect to the standard was found, Cy3glc showed the highest value, since the higher TEAC value means the higher DPPH radical scavenging activity. According to these results, and although the contribution for antioxidant activity

of LS is not high (possible due to structural complexity), the antioxidant activity of the combination of Cy3glc with LS was not affected.

Table. 11. The values of IC_{50} and TEAC samples obtained by Trolox equivalent.

Samples	TEAC	IC_{50} (µg/ml)
Trolox	-	8.87
LS	-	-
Cy3glc	2.46	3.60
Blackberry Extract	1.51	5.88
Cy3glc + LS (1:1)	2.13	4.17
Cy3glc + LS (1:4.5)	2.30	3.86

5.6. Determination of Solar Protection Factor (SPF)

As we know, solar radiations have harmful effects on human skin which are mainly caused by the ultraviolet (UV) region of the electromagnetic spectrum that play a role in causing skin cancer. Due to these facts, sunscreens substances can help to protect skin from harmful UV rays. However, it is necessary to use a very effective sunscreen to protect the skin against a wide range of UV radiation. The efficacy of a sunscreen is expressed by the sun protection factor (SPF) (Elizângela Abreu Dutra, 2004). Several factors can be effect on determination of SPF values, such as different types of solvents used, sunscreen viscosity, different types of emulsions, and the addition of other active ingredients that can increase or decrease UV absorption in sunscreens (Nalanda Baby R, 2022). Since the general idea was to formulate a sunscreen with natural compounds instead of using chemical filters which are harmful for humans and environment, natural compound such as Cy3glc and lignosulfonate were used to evaluate the amount of SPF and to what extent they can replace synthetic ones, acting at least as SPF boosters.

As an initial screening test, Cy3glc and LS were prepared at a concentration of 0.2 mg/mL in Milli-Q water (pH 4.5) and its corresponding SPF was determined according to the Mansur equation (**Table. 12**). In this proportion, the SPF values were very similar and around 15. It was also interesting to observe that the addition of both bioactives resulted in an additive value of SPF, around 30. Aiming to produce a formulation directed

to children, having attractive colours, high SPFs and based on natural bioactives, a second condition, with a high amount of LS was also tested. According to the results, free LS (4.5 mg/ 5 mL) and the combination of Cy3glc – LS (1:4.5) (**Fig. 21**) showed high SPF values (around 45 and 50, respectively). In this case the combination of both did not show the same behaviour as before. This results, highlights for the importance of testing other ratios, in order to optimize the formulation conditions.

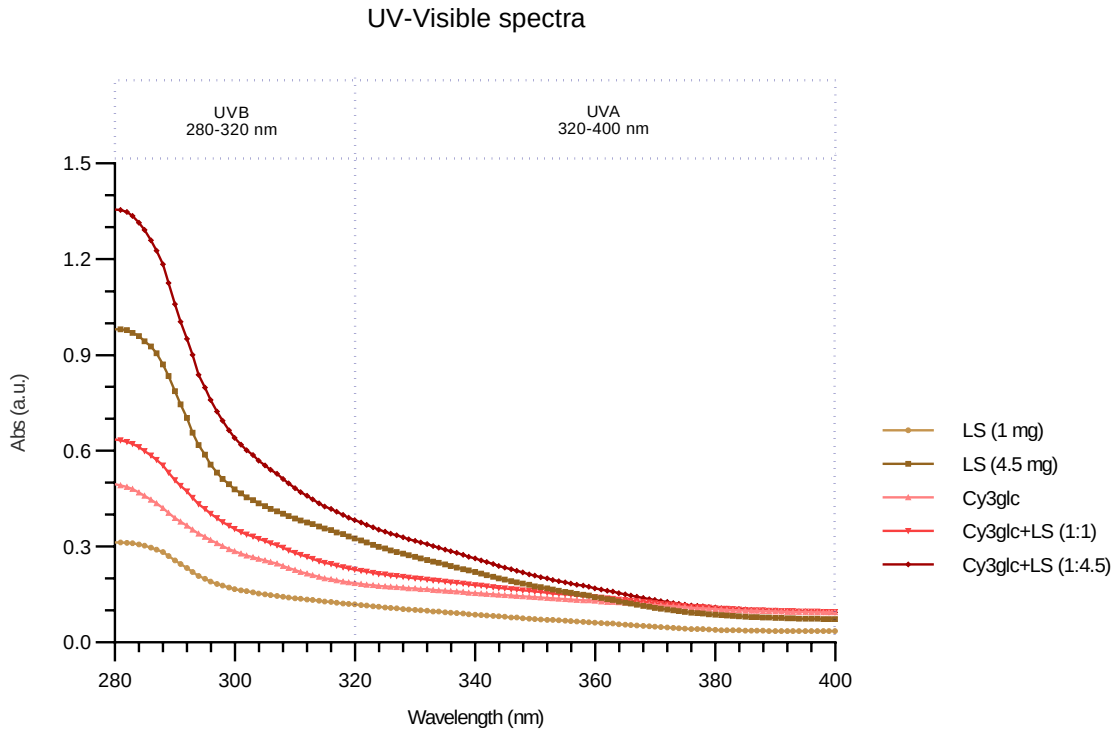

Fig. 21. Spectrum of LS (1 mg), LS (4.5 mg), Cy3glc, Cy3glc + LS (1:1), Cy3glc + LS (1:4.5).

Table. 12. In vitro solar protection factors (SPF) of Cy3glc, LS and the combination of Cy3glc+LS with colours.

Compound (mg/mL)	SPF (mean ± SD)	Colour of samples
Free LS (1 mg/ 5 mL)	14.02 ± 0.32	
Free LS (4.5 mg/ 5 mL)	44.96 ± 1.37	
Free Cy3glc (1 mg/ 5 mL)	15.15 ± 0.23	
Cy3glc – LS (1:1)	32 ± 0.57	
Cy3glc – LS (1:4.5)	50.50 ± 0.40	

5.7. Formulation

5.7.1. Gel Serum Evaluation

According to the above mentioned instructions, gel serums prepared with compounds in the following order: Free BB extract, LNP, LNP + BB, L + BB NP, Free LS, LS + BB. Based on the results obtained during 15 and 30 days' presence in (**Fig. 22**), colour changes were discernible in gel serums, particularly under light condition. Unexpectedly, lignin nanoparticles, could not preserve the stability of blackberry extract and the red pigment was no longer visible. The visible colour was the brown colour of lignin, which in compare with LNP sample, there was very similar. In contrast, in the case of combination of blackberry extract with lignin sulfonate, the red colour of blackberry extract was preserved, which means lignin sulfonate was able to interact with the flavylium form of anthocyanin and stabilize it. It should be noted that the amount of blackberry extract used in the formulation was a very small amount, since to maintain the size of nanoparticles and preventing the formation of bigger size of nanoparticles, the proportion of extract versus Kraft lignin needs to be (1:20).

Focusing our analyses on the effect of LS on Cy3glc stability, it is easy to observe that in the three conditions tested the pink colour is still visible, even after 30 days, what proves the importance of LS in the final formulation.

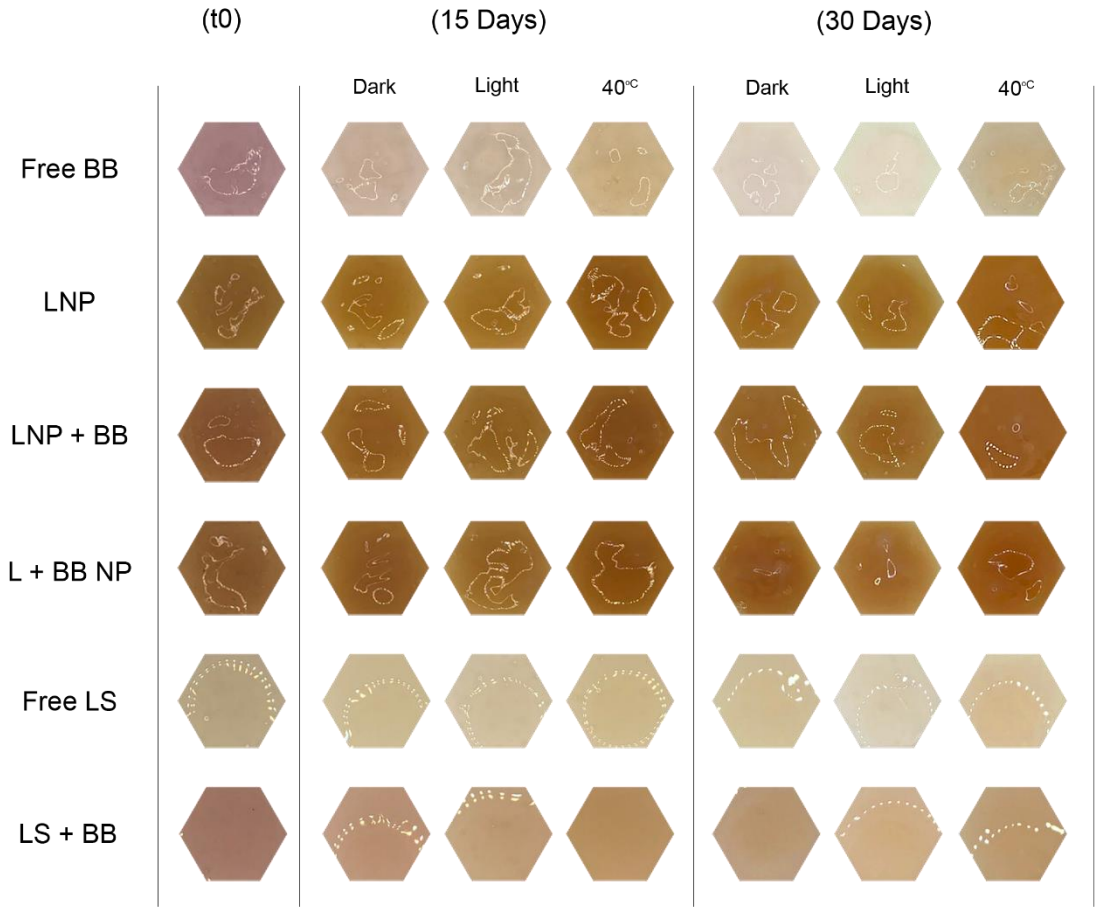

Fig. 22. The colours of gel serums in based on several compounds in different condition during 30 days.

5.7.2. Rheological Behaviour Analysis of Gel Serums (viscosity and elasticity)

The formulation was evaluated in terms of viscosity and elasticity, (**Fig. 23**). Considering obtained results of composition of gel serum, samples had fluid (liquidish) texture, which were acceptable extent. Since, gel serums have fluid/semi-fluid nature. Likewise, the viscosity and elasticity of all samples showed low values, which were normal based on the texture of gel serums. Notably, the samples with LS (Free LS and LS + BB), showed very low viscosity as well as elasticity compared with the other samples, which were more fluid. That said, being more fluid of samples with combination of LS, it might be for interaction of LS with Carbopol® 974P NF polymer that was used

in the gel serum formulation, which are high molecular weight, cross-linked polyacrylic acid polymers. They can be used to develop semisolid and oral liquid formulations with a wide range of flow and rheological properties. The polymers are highly efficient thickeners, suspending agents and stabilizers at low usage levels (0.1 - 3.0 wt%). Beside this, salts are known to cause the decrease of viscosity by reducing the charge repulsion. When adding the LS (electrolytes), a drop of viscosity was observed. It probably affected the electrostatic repulsion of the ionized carboxylic groups, which changed the rheological behaviour of the serum. In order to correct this, the quantity of lignosulfonates could be adjusted (reduce the proportion used in the serum) or, alternatively, the amount of carbomer could be slightly raised in order to achieve higher serum viscosity.

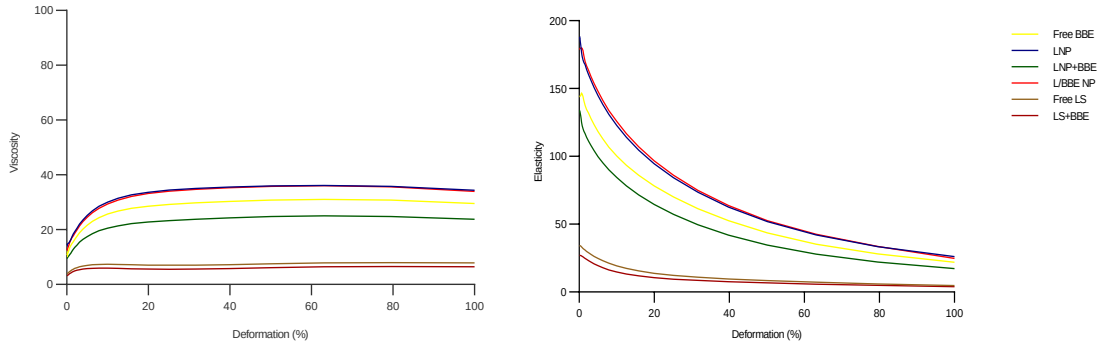

a) b)

Fig. 23. The results of viscosity and elasticity of gel serum samples in order: Free BB, LNP, LNP + BB, L + BB NP, Free LS, LS + BB.

5.7.3. Colour Measurements of Gel Serums

The obtained results presence in (**Table. 13**) in following order: LNP + BB, L + BB NP, Free BB, LS + BB samples during 15 and 30 days. Delta E, which is based on delta L*, delta a*, and delta b* colour values, all of which provide a complete numerical descriptor of the colour in a rectangular coordinate system, that the meanings are as follows: dL* represents a lightness difference between the sample and standard colours, da* represents the difference in redness or greyness between the sample and standard colours and db* denotes blueness-yellowness differences between the sample and standard colours, was measured for each sample in three different condition. In the LNP + BB, L + BB NP samples, since the colour of the samples was initially brown, due to the presence of lignin nanoparticles, it was obvious that the red BB pigment could not be

clearly detected. However, based on the values of delta E, can be say that, there was slightly difference in the colours between LNP + BB, L + BB NP, except the red colour, which was no longer visible.

On the other hand, the values of delta E in LS + BB sample was almost half of the value of delta E in Free BB sample in all storage condition and not much differences observed in the values of variation of colours over the time. Despite this, the red pigment of BB was completely recognizable, but fainter compared to zero time. With this in mind that there is a possibility of error in delta E values, due to the lack of equipment to measure the colours, which the values obtained manually.

Table. 13. The results of variation of colours in gel serums during 30 days.

Sample	Time					
	15 days			30 days		
	Dark	Light	40	Dark	Light	40
LNP + BB	11.6	11.9	11.9	12	14.2	12.9
L + BB NP	13.1	11.6	14.4	10.81	13.9	20.6
Free BB	35.9	36.9	30.6	47.4	49.9	31.4
LS + BB	23	25	20	23.6	30.4	24.4

According to the results obtained from the preparation of gel serum, such as the stability of BB extract and its combination with other compounds, as well as the texture and structure of the formulation, it was decided that the best compounds for the new formulation which had a different structure and ingredients in compared with gel serum, was the combination of LS + BB, which LS was able to increase the stability of BB extract. Overall, ligninsulfonate was the best option for using in the other formulation, which was developed to promote the stability of anthocyanins.

5.7.4. Gel-in-oil Emulsion (GELTRAP) Evaluation

By considering the obtained results of gel serums, new formulation was designed, which was emulsion type and had different ingredients, texture and properties compared to the serum gel. In this formulation, SEPIPLUS™ 400, was used as polymer, which is a

multifunctional polymer with silicone feel and glide-on spreading and with an emulsifying-stabilizing power of oil phases and compatible with solvents. As an emulsifier, which is required in the emulsion composition for stabilizing by reducing the oil-water interface tension, EASYNOV™ was used. Combination of these polymer and emulsifier with other ingredients and compounds, which were used LS and Cy3glc, leaded to formation of an emulsion with cream-like texture, which spread easily on the skin without any oily feeling on the skin.

According to the results during 30 days' present in (**Fig. 24**), and comparing the colours of the serums and emulsions, it is possible to observe that the initial colour of Cy3glc is more stable in gel-in-oil emulsions, probably due to the 3D matrix of the droplets and the complexity of this formulation composed by two different phases. It is also possible to observe that the colour obtained with gel-in-oil emulsion is around darker purple hues and in serums it was lighter. This purple coloration appears only after addition of components of the oil phase (EASYNOV) to the droplets (SEPIPLUS 400), resulting in the final formulation. The colour intensity of the combination Cy3glc with LS polymer versus Cy3glc alone, was slightly darker in the three conditions tested (dark, light and 40ºC).

On other hand, when the samples were combined with a UV filter (Neo Heliopan® AP) with or without LS the final colour turns into pink hues. This may result from a stronger interaction of flavylium cation forms of the anthocyanins with the negatively charged sulphate groups of the filter.

Generally, in these samples the presence of LS polymer was associated with a more intense colour, which can result from the huge number of sulphate groups present, coming both from the UV filter and LS (**Fig. 24**).

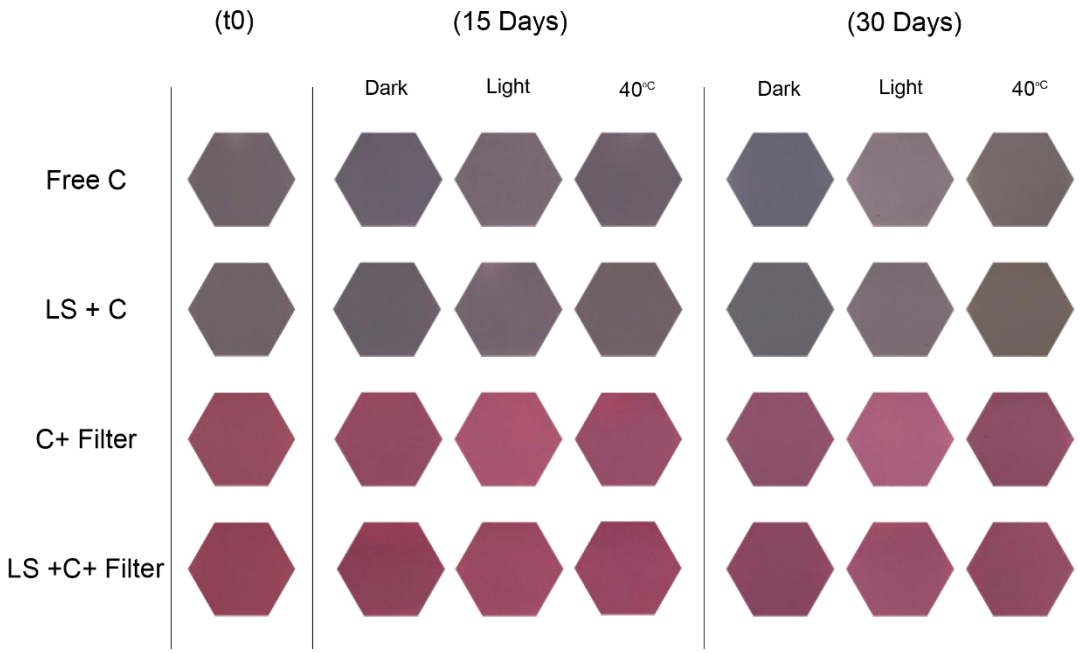

Fig. 24. The colours of gel-in-oil emulsion based on several compounds in different condition during 30 days.

5.7.5. Rheological Behaviour Analysis of Gel-in-oil Emulsion (viscosity and elasticity)

The formulation was evaluated in terms of viscosity and elasticity, (**Fig. 25**). Considering obtained results of composition of emulsion, adding Neo Heliopan® AP as a filter, which is a highly effective and photostable UVA absorber, to the free Cy3glc, decreased the viscosity, as well as the elasticity of texture compared to the free Cy3glc. In the other hand, both samples C + LS and C + LS + Filter had lower viscosity and elasticity compared to the free C and C + Filter samples, which ware not contain LS. As mentioned before, due to the structure of LS, which caused a drop in viscosity and semi-fluidization of the formulation texture. Moreover, adding extra ingredients to the formulation, may have changed the structure of the emulsion. Since, the C + LS + Filter sample had the lowest viscosity and also elasticity compared to the other samples.

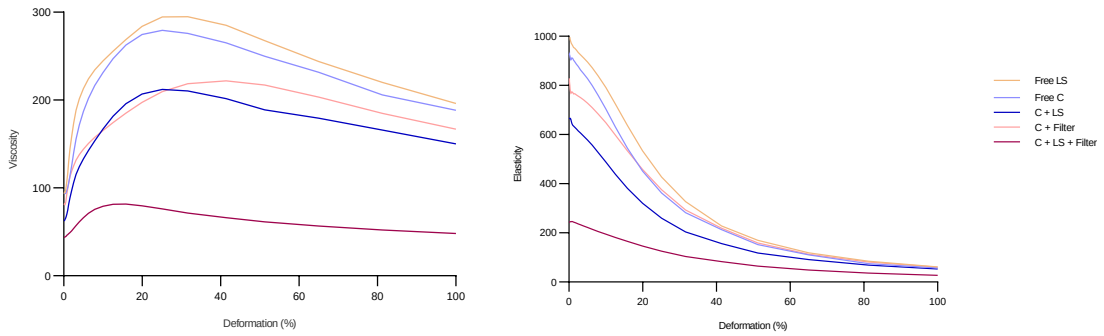

a) b)

Fig. 25. The results of viscosity and elasticity of emulsion samples in order: Free LS, Free C, C + LS, C + Filter, C + LS + Filter.

5.7.6. Colour Measurements of Gel-in-oil Emulsion

The obtained results presence in (**Table. 14**), in following order: Free Cy3glc, LS + Cy3glc, Cy3glc + Filter, LS + Cy3glc + Filter samples during 30. Delta E was measured for each sample in three different condition. The colour intensity of both Free Cy3glc and LS + Cy3glc samples were almost the same in all storage conditions, instead of under light condition, which delta E a little decreased compared to zero time over 30-days. Also, the Cy3glc + Filter and LS + Cy3glc + Filter samples, based on the delta E results, the values were similar. The most obvious difference, was the samples with filter, which completely changed the purple colour to the pink.

Table. 14. The results of variation of colours in emulsions during 30-days.

Sample	Time					
	15 days			30 days		
	Dark	Light	40	Dark	Light	40
Free C	21.4	19.8	20.9	20.6	16.5	17.3
C + LS	21.3	20.6	19.8	20.1	18.7	17.1
C + Filter	32.4	31.2	32.2	31.4	28.2	30.4
C + LS + Filter	36.9	34.9	36.9	35.8	32.2	33.5

Conclusion - Future Perspectives

With this work, it was possible to investigate some biological properties of blackberry anthocyanins and the consequences of its combination with different substances and their applicability in cosmetics industry.

Cyanidin-3-*O*-glucoside (Cy3glc), which is an anthocyanin, widely distributed among fruits and vegetables, was obtained by purification of blackberry extract with a pergentage of 92% purity.

Lignin nanoparticles (LNP) were prepared using nanoprecipitation method, in two different approaches to increase the stability of red form of Cy3glc by encapsulation. Based on obtained results for nanoparticles, which were characterized with dynamic light scattering (DLS) and electrophoretic light scattering (ELS) by measuring their average particle size (Z-average), polydispersity index (PDI) and average zeta potential (ζ), Lignin Cy3glc NPs (LNP/Cy3glc+H_2O) had similar results in compared with free LNPs results, which was selected to prepare the nanoparticles for the following assays. Beside this, by using the selected methodology the encapsulation efficiency of the red form of Cy3glc in the lignin nanoparticles in comparison with control was higher.

Regarding the combination of Cy3glc with LS, to increase the stability of anthocyanins in different storage conditions, LS was able to promote the stability of the red form of Cy3glc and also maintain the colour intensity during 30-days. Furthermore, the results of cytotoxic effects towards human epidermal keratinocytes over a period of 48 h of incubation, showed no significant cytotoxicity towards this cell line at concentrations below 2 and 0.5 mg/mL for LS and Cy3glc respectively.

Moreover, Cy3glc and the combination of Cy3glc with LS showed very high antioxidant activity compared to the Trolox (standard), what allow us to conclude that the type of interaction (electrostatic attraction) did not affect the antioxidant ability.

Also, in the determination of sun protection factor (SPF), free LS (4.5 mg/ 5 mL) and the combination of Cy3glc – LS (1:4.5), which were prepared at a concentration of 0.2 mg/mL showed high SPF values (around 45 and 50, respectively). This great rise in SPF values highlights for the importance of testing other ratios, in order to determine the optimal ratio.

In consequence, colour changes were discernible in serum gels during 15 and 30-days, particularly under light condition. Unexpectedly, lignin nanoparticles, could not preserve the stability of red pigment of blackberry extract. Nevertheless, it might be possible to promote the stability by different ratios or conditions. In contrast, the gel serum contained combination of LS with BB, could maintained the red form during 15

and 30-days, even under light condition, with the exception of texture of gel serum, which formed fluidic texture after interaction with LS. The results of viscosity and elasticity represent the structural alteration of gel serum compared to the other samples, which had drop in the both viscosity and elasticity in sample contain LS.

On the other hand, by using gel-in-oil emulsions, Cy3glc seems to be trapped in the jellified water micelles, though promoting the stability of the blue form of Cy3glc. The addition of LS to this type of matrix does not seem to have a great impact in promoting the blue colour stability or even the change to the red form. This may indicate that, the interactions with LS polymer is not favoured over micelles encapsulation. Although the rise in SPF (observed in the serums) justifies its inclusion in the final formula.

In the case of the scenario in which the substitution of UV-synthetic filter by Cy3glc+LS was followed, the change in the type of pH form that was stabilized is obviously, the formulation changes to a dark pink colour. This may result from a strong interaction of the positive charges of the anthocyanin with the negative charges of the sulphate groups present, both in the polymer and in the UV-synthetic filter. This allowed a great stability of the three member (Cy3glc+LS+UV-filter) formulation in comparison with the two-member formulation (Cy3glc+LS).

Since anthocyanins and lignins are not registered as UV-filters, their use in sunscreens would be restricted to UV-protection boosters, so the most probable formulation would be the ones containing Neo Heliopan® AP, in a reduced amount.

Accordingly, to all the obtained results, it would be important to explore additional concentrations, ratios and types of anthocyanins and lignins. Also other UV-filters could be proposed (especially the ones already reported as toxic for the environment and to humans) and other formulations could also be tested, like oil in water.

As for the additional features of the formulations, the activity towards skin enzymes responsible for wrinkle formation, or the dark spots, should be evaluated, together with the wound-healing activity.

It should also be noted that the stability assays could be prolonged in time, aiming to select the best condition to storage these formulation, giving them the long shelf-life possible.

References

(1) Kunze, G.; Schlifke, A.; Jackson, E.; Hefner, N.; Berg, K.; Vollhardt, J. A Novel, Benchmark-Centered, Eco-Impact Rating System for Sunscreens and Sunscreen Formulation Design. *Front. Environ. Sci.* **2021**, *9* (December), 1–11. https://doi.org/10.3389/fenvs.2021.727404.

(2) Matsumura, Y.; Ananthaswamy, H. N. Toxic Effects of Ultraviolet Radiation on the Skin. *Toxicol. Appl. Pharmacol.* **2004**, *195* (3), 298–308. https://doi.org/10.1016/j.taap.2003.08.019.

(3) Uif, V.; Pg, U.; Sfbujwf, U.; Mjdfotf, P. *Anatomy & Physiology*.

(4) Arda, O.; Göksügür, N.; Tüzün, Y. Basic Histological Structure and Functions of Facial Skin. *Clin. Dermatol.* **2014**, *32* (1), 3–13. https://doi.org/10.1016/j.clindermatol.2013.05.021.

(5) Biniek, K.; Levi, K.; Dauskardt, R. H. Solar UV Radiation Reduces the Barrier Function of Human Skin. *Proc. Natl. Acad. Sci. U. S. A.* **2012**, *109* (42), 17111–17116. https://doi.org/10.1073/pnas.1206851109.

(6) Chung, J. H. Photoaging in Asians. *Photodermatol. Photoimmunol. Photomed.* **2003**, *19* (3), 109–121. https://doi.org/10.1034/j.1600-0781.2003.00027.x.

(7) Tu, Y.; Quan, T. Oxidative Stress and Human Skin Connective Tissue Aging. *Cosmetics* **2016**, *3* (3), 1–12. https://doi.org/10.3390/cosmetics3030028.

(8) Pageon, H.; Zucchi, H.; Ricois, S.; Bastien, P.; Asselineau, D. UVA Exposure Combined with Glycation of the Dermis Are Two Catalysts for Skin Aging and Promotes a Favorable Environment to the Appearance of Elastosis. *J. Aging Res.* **2021**, *2021*. https://doi.org/10.1155/2021/6647773.

(9) Sample, A.; He, Y. Y. Mechanisms and Prevention of UV-Induced Melanoma. *Photodermatol. Photoimmunol. Photomed.* **2018**, *34* (1), 13–24. https://doi.org/10.1111/phpp.12329.

(10) Narayanan, D. L.; Saladi, R. N.; Fox, J. L. Ultraviolet Radiation and Skin Cancer. *Int. J. Dermatol.* **2010**, *49* (9), 978–986. https://doi.org/10.1111/j.1365-4632.2010.04474.x.

(11) Pérez-Sánchez, A.; Barrajón-Catalán, E.; Herranz-López, M.; Micol, V. Nutraceuticals for Skin Care: A Comprehensive Review of Human Clinical Studies. *Nutrients* **2018**, *10* (4), 1–22. https://doi.org/10.3390/nu10040403.

(12) Review, A. Sunscreening Agents. **2013**, *6* (1), 16–26.

(13) Kaimal, S.; Abraham, A. Sunscreens. *Indian J. Dermatol. Venereol. Leprol.* **2011**, *77* (2), 238–243. https://doi.org/10.4103/0378-6323.77480.

(14) Guan, L. L.; Lim, H. W.; Mohammad, T. F. Sunscreens and Photoaging: A Review of Current Literature. *Am. J. Clin. Dermatol.* **2021**, *22* (6), 819–828. https://doi.org/10.1007/s40257-021-00632-5.

(15) Yuan, S.; Huang, J.; Jiang, X.; Huang, Y.; Zhu, X.; Cai, Z. Environmental Fate and Toxicity of Sunscreen-Derived Inorganic Ultraviolet Filters in Aquatic Environments: A Review. *Nanomaterials* **2022**, *12* (4). https://doi.org/10.3390/nano12040699.

(16) Chatzigianni, M.; Pavlou, P.; Siamidi, A.; Vlachou, M.; Varvaresou, A.; Papageorgiou, S. Environmental Impacts Due to the Use of Sunscreen Products: A Mini-Review. *Ecotoxicology* **2022**, *31* (9), 1331–1345. https://doi.org/10.1007/s10646-022-02592-w.

(17) Pandey, K. B.; Rizvi, S. I. Plant Polyphenols as Dietary Antioxidants in Human Health and

Disease. *Oxid. Med. Cell. Longev.* **2009**, *2* (5), 270–278. https://doi.org/10.4161/oxim.2.5.9498.

(18) Amawi, H.; Ashby, C. R.; Samuel, T.; Peraman, R.; Tiwari, A. K. Polyphenolic Nutrients in Cancer Chemoprevention and Metastasis: Role of the Epithelial-to-Mesenchymal (EMT) Pathway. *Nutrients* **2017**, *9* (8). https://doi.org/10.3390/nu9080911.

(19) Arora, I.; Sharma, M.; Tollefsbol, T. O. Combinatorial Epigenetics Impact of Polyphenols and Phytochemicals in Cancer Prevention and Therapy. *Int. J. Mol. Sci.* **2019**, *20* (18). https://doi.org/10.3390/ijms20184567.

(20) Saewan, N.; Jimtaisong, A. Photoprotection of Natural Flavonoids. *J. Appl. Pharm. Sci.* **2013**, *3* (9), 129–141. https://doi.org/10.7324/JAPS.2013.3923.

(21) Panche, A. N.; Diwan, A. D.; Chandra, S. R. Flavonoids: An Overview. *J. Nutr. Sci.* **2016**, *5*. https://doi.org/10.1017/jns.2016.41.

(22) Kumar, S.; Pandey, A. K. Chemistry and Biological Activities of Flavonoids: An Overview. *Sci. World J.* **2013**, *2013*. https://doi.org/10.1155/2013/162750.

(23) Tarone, A. G.; Cazarin, C. B. B.; Marostica Junior, M. R. Anthocyanins: New Techniques and Challenges in Microencapsulation. *Food Res. Int.* **2020**, *133* (December 2019). https://doi.org/10.1016/j.foodres.2020.109092.

(24) Cheng, J.; Wei, G.; Zhou, H.; Gu, C.; Vimolmangkang, S.; Liao, L.; Han, Y. Unraveling the Mechanism Underlying the Glycosylation and Methylation of Anthocyanins in Peach. *Plant Physiol.* **2014**, *166* (2), 1044–1058. https://doi.org/10.1104/pp.114.246876.

(25) Enaru, B.; Drețcanu, G.; Pop, T. D.; Stănilă, A.; Diaconeasa, Z. Anthocyanins: Factors Affecting Their Stability and Degradation. *Antioxidants* **2021**, *10* (12). https://doi.org/10.3390/antiox10121967.

(26) Li, X.; Liu, C.; Li, Y.; Yuan, K.; Zhang, W.; Bai, D. C. Á. Z. P. Á. W. Bioactivity and Application of Anthocyanins in Skin Protection and Cosmetics : An Extension as a Functional Pigment. **2023**, *0123456789*.

(27) Kan, V.; Vargo, E.; Machover, N.; Ishii, H.; Pan, S.; Chen, W.; Kakehi, Y. Organic Primitives: Synthesis and Design of PH-Reactive Materials Using Molecular I/O for Sensing, Actuation, and Interaction. *Conf. Hum. Factors Comput. Syst. - Proc.* **2017**, *2017-May*, 989–1000. https://doi.org/10.1145/3025453.3025952.

(28) Dangles, O.; Fenger, J. A. The Chemical Reactivity of Anthocyanins and Its Consequences in Food Science and Nutrition. *Molecules* **2018**, *23* (8). https://doi.org/10.3390/molecules23081970.

(29) Gençdağ, E.; Özdemir, E. E.; Demirci, K.; Görgüç, A.; Yılmaz, F. M. Copigmentation and Stabilization of Anthocyanins Using Organic Molecules and Encapsulation Techniques. *Curr. Plant Biol.* **2022**, *29* (August 2021). https://doi.org/10.1016/j.cpb.2022.100238.

(30) Gagosian, V. S. C.; Claro, F. C.; Schwarzer, A. C. de A. P.; Cruz, J. V.; Thá, E. L.; Trindade, E. da S.; Magalhães, W. L. E.; Pestana, C. B.; Leme, D. M. The Potential Use of Kraft Lignins as Natural Ingredients for Cosmetics: Evaluating Their Photoprotective Activity and Skin Irritation Potential. *Int. J. Biol. Macromol.* **2022**, *222* (August), 2535–2544. https://doi.org/10.1016/j.ijbiomac.2022.10.037.

(31) Sipponen, M. H.; Lange, H.; Crestini, C.; Henn, A.; Österberg, M. Lignin for Nano- and Microscaled Carrier Systems: Applications, Trends, and Challenges. *ChemSusChem* **2019**,

12 (10), 2039–2054. https://doi.org/10.1002/cssc.201900480.

(32) Zhang, Y.; Naebe, M. Lignin: A Review on Structure, Properties, and Applications as a Light-Colored UV Absorber. *ACS Sustain. Chem. Eng.* **2021**, *9* (4), 1427–1442. https://doi.org/10.1021/acssuschemeng.0c06998.

(33) Widsten, P. Lignin-Based Sunscreens—State-of-the-Art, Prospects and Challenges. *Cosmetics* **2020**, *7* (4), 1–8. https://doi.org/10.3390/cosmetics7040085.

(34) Casimiro, F. M.; Costa, C. A. E.; Vega-Aguilar, C.; Rodrigues, A. E. Hardwood and Softwood Lignins from Sulfite Liquors: Structural Characterization and Valorization through Depolymerization. *Int. J. Biol. Macromol.* **2022**, *215* (June), 272–279. https://doi.org/10.1016/j.ijbiomac.2022.06.067.

(35) Liu, J.; Li, X.; Li, M.; Zheng, Y. Lignin Biorefinery: Lignin Source, Isolation, Characterization, and Bioconversion. *Adv. Bioenergy* **2022**, *7*, 211–270. https://doi.org/10.1016/bs.aibe.2022.05.004.

(36) Zevallos Torres, L. A.; Lorenci Woiciechowski, A.; de Andrade Tanobe, V. O.; Karp, S. G.; Guimarães Lorenci, L. C.; Faulds, C.; Soccol, C. R. Lignin as a Potential Source of High-Added Value Compounds: A Review. *J. Clean. Prod.* **2020**, *263*. https://doi.org/10.1016/j.jclepro.2020.121499.

(37) He, Y.; Hu, Y.; Jiang, X.; Chen, T.; Ma, Y.; Wu, S.; Sun, J.; Jiao, R.; Li, X.; Deng, L.; Bai, W. Cyanidin-3-O-Glucoside Inhibits the UVB-Induced ROS/COX-2 Pathway in HaCaT Cells. *J. Photochem. Photobiol. B Biol.* **2017**, *177* (September), 24–31. https://doi.org/10.1016/j.jphotobiol.2017.10.006.

(38) Dumitrașcu, L.; Stănciuc, N.; Aprodu, I. Encapsulation of Anthocyanins from Cornelian Cherry Fruits Using Heated or Non-Heated Soy Proteins. *Foods* **2021**, *10* (6). https://doi.org/10.3390/foods10061342.

(39) Shao, D.; Zhu, Q. H.; Liang, Q.; Wang, X.; Li, Y.; Sun, Y.; Zhang, X.; Liu, F.; Xue, F.; Sun, J. Transcriptome Analysis Reveals Differences in Anthocyanin Accumulation in Cotton (Gossypium Hirsutum L.) Induced by Red and Blue Light. *Front. Plant Sci.* **2022**, *13* (March), 1–16. https://doi.org/10.3389/fpls.2022.788828.

(40) Honda, C.; Bessho, H.; Murai, M.; Iwanami, H.; Moriya, S.; Abe, K.; Wada, M.; Moriya-Tanaka, Y.; Hayama, H.; Tatsuki, M. Effect of Temperature on Anthocyanin Synthesis and Ethylene Production in the Fruit of Earlyand Medium-Maturing Apple Cultivars during Ripening Stages. *HortScience* **2014**, *49* (12), 1510–1517. https://doi.org/10.21273/hortsci.49.12.1510.

(41) Jesus, A.; Mota, S.; Torres, A.; Cruz, M. T.; Sousa, E.; Almeida, I. F.; Cidade, H. Antioxidants in Sunscreens: Which and What For? *Antioxidants* **2023**, *12* (1). https://doi.org/10.3390/antiox12010138.

(42) Dutra, E. A.; Da Costa E Oliveira, D. A. G.; Kedor-Hackmann, E. R. M.; Miritello Santoro, M. I. R. Determination of Sun Protection Factor (SPF) of Sunscreens by Ultraviolet Spectrophotometry. *Rev. Bras. Ciencias Farm. J. Pharm. Sci.* **2004**, *40* (3), 381–385. https://doi.org/10.1590/S1516-93322004000300014.

(43) Baby, N.; Chakraborty, S. Determination of Sun Protection Factor (SPF) for Various Sunscreens by UV Spectrophotometry. *Ymer* **2022**, *21* (11), 483–491.